Myelin regulatory factor drives remyelination in multiple sclerosis

Acta Neuropathologica
Myelin Regulatory Factor Drives Remyelination in Multiple Sclerosis
--Manuscript Draft--

Manuscript Number:	ANEU-D-17-00179R2
Full Title:	Myelin Regulatory Factor Drives Remyelination in Multiple Sclerosis
Article Type:	Original Paper
Keywords:	Remyelination; multiple sclerosis; MYRF; oligodendrocyte; Cre-loxP.
Corresponding Author:	Wolfram Tetzlaff University of British Columbia Vancouver, British Columbia CANADA
Corresponding Author Secondary Information:	
Corresponding Author's Institution:	University of British Columbia
Corresponding Author's Secondary Institution:	
First Author:	Greg J. Duncan
First Author Secondary Information:	
Order of Authors:	Greg J. Duncan
	Jason R. Plemel
	Peggy Assinck
	Sohrab B. Manesh
	Fraser G.W. Muir
	Ryan Hirata
	Matan Berson
	Jie Liu
	Michael Wegner
	Ben Emery
	G.R. Wayne Moore
	Wolfram Tetzlaff
Order of Authors Secondary Information:	

Abstract: Remyelination is limited in the majority of multiple sclerosis (MS) lesions despite the presence of oligodendrocyte precursor cells (OPCs) in most lesions. This observation has led to the view that a failure of OPCs to fully differentiate underlies remyelination failure. OPC differentiation requires intricate transcriptional regulation, which may be disrupted in chronic MS lesions. The expression of few transcription factors have been

differentially compared between remyelinating lesions and lesions refractory to remyelination. In particular, the oligodendrocyte transcription factor myelin regulatory factor (MYRF) is essential for myelination during development, but its role during remyelination and expression in MS lesions is unknown. To understand the role of MYRF during remyelination, we genetically fate mapped OPCs following lysolecithin-induced demyelination of the corpus callosum in mice and determined that MYRF is expressed in new oligodendrocytes. OPC-specific Myrf deletion did not alter recruitment or proliferation of these cells after demyelination, but decreased the density of new glutathione S-transferase π positive oligodendrocytes. Subsequent remyelination, in both the spinal cord and corpus callosum is highly impaired following Myrf deletion from OPCs. Individual OPC-derived oligodendrocytes, produced in response to demyelination, showed little capacity to express myelin proteins following Myrf deletion. Collectively, these data demonstrate a crucial role of MYRF in the transition of oligodendrocytes from a premyelinating to a myelinating phenotype during remyelination. In the human brain, we find that MYRF is expressed in NogoA and CNP-positive oligodendrocytes. In MS, there was both a lower density and proportion of oligodendrocyte lineage cells and NogoA+ oligodendrocytes expressing MYRF in chronically demyelinated lesions compared to remyelinated shadow plaques. The relative scarcity of oligodendrocyte lineage cells expressing MYRF in demyelinated MS lesions demonstrates, for the first time, that chronic lesions lack oligodendrocytes that express this necessary transcription factor for remyelination and supports the notion that a failure to fully differentiate underlies remyelination failure.

1 **Title: Myelin Regulatory Factor Drives Remyelination in Multiple Sclerosis**

2 **Authors:** Greg J. Duncan[1,2], Jason R. Plemel[6], Peggy Assinck[1,3], Sohrab B. Manesh[1,3], Fraser G.W. Muir[1,4,], Ryan
3 Hirata[1], Matan Berson[1], Jie Liu[1], Michael Wegner[8], Ben Emery[9,10], G.R. Wayne Moore[1,4,7] and Wolfram Tetzlaff[1,2,5].

4 **Affiliations:** [1] International Collaboration on Repair Discoveries (ICORD), University of British Columbia (UBC),
5 Vancouver, BC, Canada

6 [2] Department of Zoology

7 [3] Graduate Program in Neuroscience

8 [4] Pathology and Laboratory Medicine

9 [5] Department of Surgery

10 [6] Department of Clinical Neurosciences, Hotchkiss Brain Institute, University of Calgary, Calgary, Alberta Canada

11 [7] Vancouver Hospital and Health Sciences Centre

12 [8] Institut für Biochemie, Emil-Fischer-Zentrum, Friedrich-Alexander-Universität Erlangen-Nürnberg, Erlangen,
13 Germany.

14 [9] School of Medicine, Jungers Center for Neurosciences Research, Oregon Health and Science University, U.S.A.

15 [10] Department of Anatomy and Neuroscience, University of Melbourne, Australia.

16 ***Corresponding Author:**
17 Wolfram Tetzlaff, MD, PhD.
18 John and Penny Ryan British Columbia Leadership Chair in Spinal Cord Research
19 Professor, Departments of Zoology and Surgery
20 Director ICORD (International Collaboration on Repair Discoveries)
21 University of British Columbia
22 Blusson Spinal Cord Centre
23 818 West 10th Avenue
24 Vancouver, BC, V5Z 1M9
25 *Phone:* 604 675 8848
26 *Fax:* 604 675 8820
27 *Email:* tetzlaff@icord.org
28
29

30

31

32

33

34

35

36

37

38

1

Abstract

Remyelination is limited in the majority of multiple sclerosis (MS) lesions despite the presence of oligodendrocyte precursor cells (OPCs) in most lesions. This observation has led to the view that a failure of OPCs to fully differentiate underlies remyelination failure. OPC differentiation requires intricate transcriptional regulation, which may be disrupted in chronic MS lesions. The expression of few transcription factors have been differentially compared between remyelinating lesions and lesions refractory to remyelination. In particular, the oligodendrocyte transcription factor myelin regulatory factor (MYRF) is essential for myelination during development, but its role during remyelination and expression in MS lesions is unknown. To understand the role of MYRF during remyelination, we genetically fate mapped OPCs following lysolecithin-induced demyelination of the corpus callosum in mice and determined that MYRF is expressed in new oligodendrocytes. OPC-specific *Myrf* deletion did not alter recruitment or proliferation of these cells after demyelination, but decreased the density of new glutathione *S*-transferase π positive oligodendrocytes. Subsequent remyelination, in both the spinal cord and corpus callosum is highly impaired following *Myrf* deletion from OPCs. Individual OPC-derived oligodendrocytes, produced in response to demyelination, showed little capacity to express myelin proteins following *Myrf* deletion. Collectively, these data demonstrate a crucial role of MYRF in the transition of oligodendrocytes from a premyelinating to a myelinating phenotype during remyelination. In the human brain, we find that MYRF is expressed in NogoA and CNP-positive oligodendrocytes. In MS, there was both a lower density and proportion of oligodendrocyte lineage cells and NogoA+ oligodendrocytes expressing MYRF in chronically demyelinated lesions compared to remyelinated shadow plaques. The relative scarcity of oligodendrocyte lineage cells expressing MYRF in demyelinated MS lesions demonstrates, for the first time, that chronic lesions lack oligodendrocytes that express this necessary transcription factor for remyelination and supports the notion that a failure to fully differentiate underlies remyelination failure.

Keywords: remyelination, multiple sclerosis, MYRF, oligodendrocyte, Cre-loxP

2

Introduction

Multiple sclerosis (MS) is characterized by inflammatory CNS demyelination and is one of the most common causes of chronic motor disability in young adults [60]. Remyelination occurs in MS [49, 51], which is sufficient to restore conductance in experimental models [55] and potentially protect axons from degeneration [16, 26, 32, 44]. However, remyelination is often incomplete [46] with a lower percentage of remyelinating shadow plaques relative to demyelinated plaques at all ages [20] despite fewer acute inflammatory lesions with disease chronicity [19, 36]. While oligodendrocyte precursor cells (OPCs) and some premyelinating oligodendrocytes are found within chronically demyelinated MS lesions [7, 34, 61, 62], these lesions contain few oligodendrocytes capable of remyelination. This has led to the hypothesis that a failure of OPCs to fully differentiate causes remyelination failure in MS [14, 15, 34]. Oligodendrocyte differentiation requires intricate transcriptional regulation during development, but the role of many key transcription factors remain untested during remyelination [12]. We hypothesized that remyelination failure could result if the chronic lesion environment inhibits the expression of essential transcription factor(s) needed for oligodendrocyte differentiation or myelin gene expression.

Myelin regulatory factor (MYRF) is a transcription factor expressed in oligodendrocytes [5, 6, 11] and is essential for developmental myelination [11]. MYRF can directly bind putative enhancer sequences of myelin genes, such as *Mbp* and *Plp,* to induce their expression [5] and together with the transcription factor Sox10, synergistically promote myelin gene expression [11, 25]. Genetic deletion of *Myrf* during development results in a near complete failure to differentiate into late-stage myelinating oligodendrocytes yet does not overtly affect the specification of OPCs [11]. Therefore, *Myrf* deletion during development mirrors what is observed in chronically demyelinated MS lesions; OPCs are maintained within the CNS but cannot fully differentiate. At this time, no study has investigated the role of MYRF during remyelination nor its expression in MS lesions.

Here, we examined the function of MYRF during remyelination. By genetically fate mapping OPCs following lysolecithin (LPC) demyelination in the corpus callosum of mice, we found that MYRF was expressed in new oligodendrocytes. When *Myrf* was deleted in OPCs, their recruitment and proliferation within the lesion were not affected, but their capacity to differentiate into new oligodendrocytes was greatly diminished. OPC differentiation stalled at the premyelinating stage with recombined cells unable to express myelin proteins, ultimately inhibiting remyelination in both the corpus callosum and in the spinal cord. In human white matter, MYRF was expressed in Sox10+ oligodendrocyte lineage cells, which often co-labelled with the mature

3

93   oligodendrocyte marker NogoA. In the centres of chronic active MS lesions, there was a reduction in the density of

94   MYRF+Sox10+ cells relative to both shadow plaques and normal-appearing white matter (NAWM). Additionally,

95   fewer Sox10+ oligodendrocyte lineage cells, and Sox10+NogoA+ oligodendrocytes expressed MYRF in the lesion

96   centres relative to shadow plaques, indicating these cells lacked expression of a necessary transcription factor for

97   differentiation and myelination. Collectively, these data demonstrate that *Myrf* is essential for remyelination in the

98   rodent CNS and its failure to be expressed in oligodendrocytes in chronic MS lesions is associated with

99   remyelination failure.

100

101   **Materials and Methods**

102   *Transgenic Mice and Experimental Design*

103   Myrf$^{fl/fl}$ mice [11], which have LoxP inserted around exon 8 of *Myrf*, were crossed with PDGFRα-CreERT2

104   mice [52]. The Cre-mediated recombination of *Myrf* in the Myrf$^{fl/fl}$ mice was predicted to result in the production of

105   a truncated protein that lacks the DNA-binding domain found in exon 8 and the C-terminus of the protein due to a

106   frame shift, ultimately making the protein non-functional [11, 40]. Myrf$^{fl/fl}$ PDGFRα-CreERT2 (P-Myrf$^{fl/fl}$) mice

107   were used to induce selective recombination and *Myrf* deletion in a portion of platelet-derived growth factor receptor

108   α (PDGFRα)+ cells and Myrf$^{fl/wt}$ PDGFRα-CreERT2 (P-Myrf$^{fl/wt}$) littermates were used as controls. Myrf$^{fl/wt}$ mice

109   demonstrate no phenotype following recombination compared to mice wildtype for *Myrf* [11, 40]. For genetic fate

110   mapping experiments, Myrf$^{fl/fl}$ PDGFRα-CreERT2 lines were subsequently crossed with Rosa26R-eYFP (YFP) Cre-

111   inducible reporter mice [56] or ROSA26-mGFP (mT/mG) [42] to induce, via Cre-mediated recombination,

112   cytoplasmic or membrane-tethered fluorescence, respectively. Both Cre and inducible reporter genes were

113   heterozygous in all experiments. All animals were genotyped prior to experiments via standard protocols. Myrf$^{fl/fl}$

114   mice were also crossed with PLP-CreERT2 and Rosa26-YFP mice to produce Myrf$^{fl/wt}$ and Myrf$^{fl/fl}$ PLP CreERT2

115   Rosa26-YFP mice to induce recombination in oligodendrocytes following tamoxifen injection.

116   *Tamoxifen administration*

117   Tamoxifen (T5648, Sigma) was dissolved in corn oil (C8267, Sigma) at 20mg/ml. P-Myrf^{fl} mice received

118   intraperitoneal injections (100mg/kg) once daily for five days starting two days prior to lysolecithin demyelination.

119   For Myrf$^{fl/wt}$ PLP CreERT Rosa26 YFP and Myrf$^{fl/fl}$ PLP CreERT Rosa26 YFP mice, 4-hydroxytamoxifen (H7904,

120   Sigma) was dissolved in corn oil at 10mg/mL and 1mg was administered by intraperitoneal injection once per day

4

121 for five consecutive days. Tamoxifen improves the speed of remyelination at relatively low doses (0.5-2.0

122 mg/kg)[22] and results in cellular stress at high doses (75mg/kg) indicated by the upregulation of the Atf3

123 transcription factor [9]. To control for tamoxifen-mediated effects, all mice were treated with the same tamoxifen

124 regiment except for a group of mice for qPCR and another for lesion size analysis at 3 days post lesion (DPL) which

125 were injected with corn oil alone. We found that tamoxifen had no effect on lesion size at 3 DPL (tamoxifen treated

126 0.473 ± 0.099 mm^2 versus non-tamoxifen treated $0.376 \pm .027$ mm^2, P=0.355 Student's T-Test) suggesting that

127 tamoxifen does not alter the susceptibility to lysolecithin-mediated demyelination.

128 *Real-time quantitative PCR*

129 2mm^3 blocks of the anterior corpus callosum and cortex were collected from P-Myrf$^{fl/fl}$ and P-Myrf$^{fl/wt}$ mice

130 12 days after the last tamoxifen or oil injection and flash frozen. RNA was extracted and reversed transcribed as

131 previously described [48]. Primers for recombined *Myrf* [31] were normalized relative to β-actin and CT values were

132 determined by automatic baseline and auto-threshold. ΔΔCT method was used to compare relative gene expression

133 between groups [38].

134 *Lysolecithin demyelination*

135 1% lysophosphatidylcholine (lysolecithin L1381, Sigma) was dissolved in sterile phosphate-buffered saline

136 (PBS) by sonication. Mice were deeply anaesthetized using a 3% isoflurane-oxygen mixture (Baxter) and a small

137 hole was drilled with a dentist drill to allow for the insertion of a glass capillary attached to a 5 µL Hamilton syringe

138 into the brain tissue. A total of 2µL was injected at a rate of 50nL/min by a pump (Precision Scientific Instruments)

139 into the corpus callosum at the coordinates 1.4mm anterior to bregma, 1mm lateral of bregma and 2.1mm deep from

140 the cortical surface. The glass capillary was retained in place for at least five minutes post injection to reduce reflux

141 along the needle track. Mice received buprenorphine twice daily to alleviate pain (0.03mg/kg) for the first two days

142 post-surgery and 1mL Ringer's solution. The overlying skin was sutured. For lysolecithin demyelination of the

143 cervical spinal cord, surgeries were conducted as above with the following differences. A laminectomy of the C4

144 vertebrae was performed with fine surgical rongeurs. Injections were placed at a 30 degree angle relative to vertical

145 and just lateral to the midline in the dorsal column to a depth of 0.5mm ventral to the dorsal surface. A total of

146 0.5µL of lysolecithin was injected at a rate of 50nL/min. The overlying musculature and skin were sutured.

147 *Tissue processing*

148   For immunohistochemical analysis of tissue, mice were deeply anaesthetized and transcardially perfused

149 with PBS followed by 4% paraformaldehyde (04042, Fisher Scientific). Spinal cords or brains were dissected and

150 postfixed in paraformaldehyde for either eight hours or overnight for brains. Tissue was then cryoprotected in

151 ascending sucrose solutions before being embedded in OCT, frozen, and stored at -80° Celsius. Tissue was sectioned

152 coronally at 20µm thickness using a cryostat (HM-525, Thermo Scientific) and sections were thaw-mounted onto

153 slides (12-550-15, Fisher Scientific).

154   To prepare tissue for electron microscopy, mice were deeply anaesthetized then perfused with 0.01M PBS

155 before receiving 1% glutaraldehyde (16221, Electron Microscopy Sciences) with 4% paraformaldehyde at 4° C. The

156 area of demyelination was immediately dissected into $1mm^3$ cubes and postfixed in 2% glutaraldehyde. Tissue was

157 washed three times in 0.1M cacodylate buffer with 5.3mM $CaCl_2$ before being placed in 1% osmium tetroxide

158 (19190, Electron Microscopy Sciences) with 1.5% potassium ferrocyanide (BDH) for 1.5 hours. Tissue was then

159 dehydrated through ascending alcohol washes before embedding in Spurr resin.

160 *Immunohistochemistry*

161   Slides were thawed prior to staining and rehydrated with PBS. Sections were blocked using 10% donkey

162 serum dissolved in PBS with 0.1% Triton. Primary antibodies (Supplementary Table 1) were applied overnight at

163 room temperature in a humid chamber, washed, then appropriate donkey Dylight or Alexa Fluor secondary

164 antibodies (Jackson ImmunoResearch Laboratories, Inc) were applied for two hours. Slides were subsequently

165 washed and coverslipped using Fluoromount-G (0100-01, Southern Biotech). Prior to myelin stains, delipidation

166 was performed using ascending and descending ethanol washes followed by PBS washes before the blocking step.

167 *Cell counts and quantifications on mouse tissue*

168   Imaging on mice was performed on a Zeiss Axio-Observer M1 inverted spinning disc confocal microscope

169 using Zen 2011 or Zen 2 software. Tiled confocal merged images of the entire demyelinated zone in the corpus

170 callosum were captured with a 40x oil immersion objective (numerical aperture 1.3) using a distance of 1µm

171 between the individual optical sections. For cell counts, the lesion was defined by either the absence or obvious

172 damage of myelin based on myelin basic protein (MBP) or 2',3'-cyclic-nucleotide 3'-phosphodiesterase (CNP)

173 stains. The lesion area was defined by the presence of the astrocyte scar (increased GFAP+ density) for the analysis

174 of the contribution of recombined cells to remyelination and analyses of the number of nodes of Ranvier. Five to

175 seven sections were analyzed per animal beginning with the lesion epicenter. For analyses of the oligodendrocyte

176 density in the uninjured CNS, the corpus callosum contralateral to the lysolecithin injection were examined for

177 PDGFRα+ and glutathione s-tranferases pi isoform (GSTπ)+ cells in the area dorsal of the ventricle.

178 To quantify node of Ranvier density systematic random sampling was conducted in the lesion and nodes of

179 Ranvier were counted in 50µm x 50µm areas. Mature nodes of Ranvier were defined as punctate clusters of

180 Ankyrin-G (AnkG) flanked by two punctate Caspr-positive paranodes [41]. Typically, over 1000 nodes were

181 counted over 5-6 sections per animal. The density of SMI312+ axons were thresholded on ImageJ (NIH) and

182 quantified as a percentage of lesion area. The volume of demyelinated tissue in P-Myrf$^{fl/fl}$ YFP and P-Myrf$^{fl/wt}$ YFP

183 was examined by manually outlining the area of the intact corpus callosum that was MBP-negative.

184 To determine the area of demyelination that had been remyelinated by recombined cells in Myrf$^{fl/fl}$

185 PDGFRαCreERT2 mT/mG and Myrf$^{fl/wt}$ PDGFRαCreERT2 mT/mG mice, the lesion was imaged for GFP, MBP

186 and GFAP. The ImageJ plugin 'RG2B Colocalization' was used to determine the area of GFP and MBP

187 colocalization within the manually defined GFAP+ lesion.

188 *Electron microscopy*

189 Resin blocks with lysolecithin lesions were sampled every 250µm to determine the lesion epicenter. At the

190 epicenter, 1µm semithin sections were cut on an ultramicrotome (Ultracut E, Reichert-Jung) and stained briefly in a

191 1% toluidine blue and 2% borax solution then coverslipped with Permount (SP15, Fisher Scientific). Rank analysis

192 was performed [30] by two blinded raters on images of semithin sections of the whole dorsal column taken with a

193 63x oil immersion objective (numerical aperture 1.3) on a Zeiss, Axio Imager.M2 microscope. Each section was

194 scored independently for the presence of thinly myelinated axons. When discrepancies in the ranking occurred, the

195 average score was taken. For electron microscopy, ultrathin (90nm) sections of the lesion epicenter were collected

196 and stained with Reynold's lead citrate and uranyl acetate to enhance contrast then imaged at 10000-12500x primary

197 magnification on a Zeiss EM910.

198 *Human tissue analysis*

199 Human brain tissue was used with the approval of the UBC Clinical Research Ethics Board of the

200 University of British Columbia (H01-70430). Patient information as well as the number of lesions analyzed for non-

201 MS controls and MS patients is displayed in Supplementary Table 2. Sections (5µm) from formalin-fixed paraffin-

202 embedded tissue were obtained on microtome (1512, Leitz) and all lesions were stained on adjacent slides with luxol

203 fast blue (LFB), and immunohistochemically for class II human leukocyte antigen (HLA II), MBP and CNP for

7

204 lesion classification according to histological criteria [4, 59]. Only lesions within the subcortical or periventricular

205 white matter were examined. NAWM was examined at least 1.0 cm distant from a lesion in an area lacking

206 inflammation. For immunohistochemical staining, slides were first deparaffinized then antigen retrieval was

207 performed by heating slides in pH 6.0 10mM sodium citrate buffer for ten minutes. Blocking was performed in 10%

208 normal donkey serum in PBS Tween. Primary antibodies were applied overnight in a humid chamber before

209 washing and applying appropriate Alexa Fluor conjugated secondary antibodies (Jackson ImmunoResearch

210 Laboratories) at 1:200 for two hours. Slides were washed with PBS then stained with 0.30% (0.15% in slides with

211 NogoA) Sudan black in 70% ethanol (4197-25-5, Sigma) for three minutes before being washed again in PBS and

212 coverslipped with Fluoromount-G. An adjacent control slide for each lesion was stained simultaneously with

213 secondary antibodies, Hoechst (1:10000) and Sudan black but lacked primary antibodies for comparison of

214 background fluorescence. Cells were considered positive only if their fluorescence was substantially higher than

215 background fluorescence as assessed on control slides imaged with the same exposure settings. Systematic random

216 sampling was used within the lesion area manually defined on the Zen 2 software by Sudan black staining and cross-

217 referenced with adjacent slides with HLA II and LFB staining. At least twenty 100µm x 100µm areas were

218 examined in all lesions. Chronic lesions had 60 100µm x 100µm areas counted to increase the likely of detecting

219 oligodendrocyte lineage cells.

220 *Statistical Analyses*

221 Statistical analyses were conducted on Statistical Package for Social Sciences software (IBM) and

222 Graphpad (Prism) version 6.0. Parametric statistics were used assuming data met requirements for normality, tested

223 by the Shapiro-Wilk test. For comparisons between two normally distributed groups, Student's t-test was used with

224 or without the Welch correction depending on whether assumptions of the homogeneity of variance were met,

225 analyzed by with Levene's test. The Mann-Whitney U-test was used to compare P-Myrf$^{fl/fl}$ to controls when the data

226 was not normally distributed or was ordinal. A one-way ANOVA followed by Tukey's or Tamhane's *post hoc* test

227 depending on whether there was equal homogeneity of variance between groups was used to compare three or more

228 groups at one time point. For comparisons of cell counts between groups at different time points post-lysolecithin

229 injection, a two-way ANOVA was run followed by Tukey's *post hoc* test. A unit was considered an individual

230 animal or MS lesion. Individuals performing surgeries, cell counts and imaging were blinded to mouse genotype by

231 a third party. For all tests, statistical significance was obtained if P<0.05 and all statistical tests were two-tailed. Data

8

232   are presented as the mean ± standard error of the mean. On graphs ns = not statistically significant, * = P≤0.05, ** =

233   P≤0.01, ***P≤0.001 unless otherwise specified.

234

235   **Results**

236   *MYRF is expressed in new oligodendrocytes during remyelination*

237   The role of many oligodendrocyte transcription factors remains unstudied during remyelination, including

238   MYRF. To investigate if MYRF is expressed in new oligodendrocytes during remyelination, we fate mapped OPCs

239   using a tamoxifen-inducible Cre reporter line (Rosa26-eYFP) [56] in conjunction with an OPC inducible Cre-

240   recombinase (PDGFRα-CreERT2) [52]. Mice were heterozygous for the *Myrf* floxed allele (Myrf$^{fl/wt}$). *Myrf* is

241   haplosufficient and its function in oligodendrocytes is unchanged versus mice with two copies of the gene [11]. To

242   induce reproducible demyelination, mice received an injection of lysolecithin into the genu of the corpus callosum

243   (Fig. 1a). Remyelination following lysolecithin demyelination involves a stereotypic evolution [13]. OPCs

244   proliferate and are recruited in the first 5 DPL, which is followed by prominent oligodendrocyte differentiation

245   between 5-10 DPL and remyelination by ~14 DPL (Fig. 1a). Lysolecithin was very toxic to oligodendrocyte lineage

246   cells and the majority of MYRF+ cells were lost at 3 DPL (Fig. 1b). However, by 7 and 14 DPL, MYRF+ cells

247   increased in density relative to 3 DPL (Fig. 1c). Recombined yellow fluorescent protein positive (YFP+) cells rarely

248   expressed MYRF at 3 DPL (10.28 ± 4.16%) but by 7 DPL 37.5% ± 4.00% of recombined cells expressed MYRF.

249   To identify the cells expressing MYRF during remyelination, we assessed co-immunoreactivity of YFP with CC1

250   for oligodendrocytes (Fig. 1e) and PDGFRα for OPCs (Fig. 1f). While MYRF was not found expressed in OPCs

251   (Fig. 1f), new oligodendrocytes (YFP+CC1+) were frequently observed to express nuclear MYRF staining at 7 DPL

252   in P-Myrf$^{fl/wt}$ YFP mice (Fig. 1e). Collectively, MYRF+ cells were lost after lysolecithin-induced demyelination,

253   and OPCs differentiate into new oligodendrocytes that express MYRF during remyelination.

254

255   *Inducible deletion of Myrf from OPCs is sufficient to reduce MYRF expression within new oligodendrocytes*

256   To uncover MYRF's function during remyelination, Myrf$^{fl/fl}$ PDGFRα CreERT2 Rosa26-eYFP mice (P-

257   Myrf$^{fl/fl}$ YFP) were produced to delete *Myrf* and visualize OPCs and their progeny when tamoxifen had been

258   administered. New oligodendrocytes (YFP+CC1+) in P-Myrf$^{fl/fl}$ YFP mice were less likely to express MYRF (Fig.

259   1e, g). Total MYRF density in P-Myrf$^{fl/fl}$ YFP mice declined by 32% at 7 DPL and 45% at 14 DPL relative to

9

260 controls (Supplementary Fig. 1S e). The MYRF antibody used here, raised against the N-terminus, should be

261 capable of detecting the predicted truncated, non-functional protein product of the recombined allele. Nevertheless,

262 the protein produced appears to be unstable and is only weakly detected in most recombined oligodendrocytes ([31]

263 and Supplementary Fig. S1, 2, Fig. 1e, g). To explicitly determine if the inducible knockout effectively recombined

264 *Myrf*, we examined the relative expression using a PCR primer sequence specific to recombined *myrf* mRNA

265 lacking exon 8 [31]. P-Myrf$^{fl/fl}$ mice had increased levels of recombined *myrf* in the brain compared to P-Myrf$^{fl/fl}$

266 mice without tamoxifen (Fig. 1h). Taken together, conditional deletion of *Myrf* in OPCs was effective at reducing

267 MYRF expression within new oligodendrocytes during remyelination.

268

269 *MYRF is not required for recruitment or proliferation of OPCs but is crucial for their complete maturation into new*

270 *oligodendrocytes following demyelination.*

271   OPC recruitment is crucial for timely remyelination [47], and OPC proliferation is required for sustained

272 oligodendrogenesis [53]. To determine directly if OPC recruitment or proliferation was altered by *Myrf* deletion,

273 sections from P-Myrf$^{fl/fl}$ YFP and P-Myrf$^{fl/wt}$ YFP mice were examined for PDGFRα and the cell proliferation

274 marker Ki67 to label cells in active stages of the cell cycle [54]. Both the non-recombined PDGFRα+ OPCs and

275 recombined subpopulation expressed Ki67 after lysolecithin demyelination (Fig. 2a, d, e). *Myrf* deletion from OPCs

276 did not alter the density of OPCs (Fig. 2b), the density of proliferating OPCs (Fig. 2c), the overall percentage of

277 proliferating OPCs (Fig. 2f) or proliferation within recombined OPCs (Fig. 2g). Therefore, MYRF is not required

278 for OPC proliferation or recruitment to demyelinated lesions.

279   To determine how *Myrf* deletion from OPCs affects their subsequent differentiation and maturation during

280 remyelination, we first examined whether recombined cells continued to express the OPC marker PDGFRα or have

281 differentiated and express CC1 (Fig. 3a). At 3, 7 and 14 DPL the percentage of recombined cells that expressed CC1

282 or PDGFRα did not differ between P-Myrf$^{fl/fl}$ YFP and P-Myrf$^{fl/wt}$ mice (Fig. 3b, c). Given that CC1 was expressed

283 early after lysolecithin-induced demyelination before the onset of significant remyelination (Supplementary Fig.

284 S3), we reasoned that MYRF might be dispensable for early differentiation of oligodendrocytes into a

285 premyelinating phenotype, but crucial for the expression of later markers of oligodendrocyte differentiation. At 7

286 DPL, a time point in which CC1+ cells were abundant within the lesion, staining with the oligodendrocyte marker

287 GSTπ, indicates that GSTπ+ cells are largely absent from the lesion (Supplementary Fig. S3). However, by 14 DPL,

10

288 GSTπ+ cells were found throughout the lesion (Fig. 3d), suggesting GSTπ labels a later stage of oligodendrocyte

289 development relative to CC1. Recombined cells from P-Myrf$^{fl/fl}$ YFP and P-Myrf$^{fl/wt}$ YFP mice were examined for

290 GSTπ and CNP expression at 7 and 14 DPL (Fig. 3d, e, f). In P-Myrf$^{fl/fl}$ YFP mice, a lower percentage of

291 recombined cells expressed CNP (Fig 3g) and GSTπ (Fig. 3h) relative to controls at 14 DPL. There was also an

292 overall decrease in the total density of GSTπ+ cells in P-Myrf$^{fl/fl}$ YFP mice, despite recombination in only a portion

293 of OPCs (Fig. 3i). Thus during remyelination, markers expressed later in the differentiation of OPCs into

294 oligodendrocytes, like GSTπ, were increasingly diminished relative to early differentiation markers like CC1

295 following *Myrf* deletion.

296   Decreased expression of GSTπ could not be accounted for by increased differentiation of OPCs into other

297 cell types including astrocytes, as *Myrf* deletion did not increase the proportion of cells expressing GFAP during

298 remyelination and over 95% of recombined cells have nuclear Olig2 suggesting they remain within the

299 oligodendrocyte lineage (Supplementary Fig. S4). In sections from a complimentary cohort of P-Myrf$^{fl/fl}$ and P-

300 Myrf$^{fl/wt}$ mice lacking the Rosa26-eYFP inducible reporter, sections were co-stained with Olig2 in combination with

301 stage-specific markers of oligodendrocyte maturation to ensure that changes in OPC and oligodendrocyte densities

302 could not be attributable to labelling of CC1 or PDGFRα in other cell types (Supplementary Fig. S5). Like in

303 inducible reporter-positive mice, we found no change in OPC recruitment (Supplementary Fig. S5 b, e), or the onset

304 of differentiation (Olig2+CC1+ cells) at 5 DPL but a decrease in Olig2+ density and Olig2+CC1+ oligodendrocytes

305 at 10 DPL (Supplementary Fig. S5 d, f). Collectively, these data indicate MYRF is not required for OPC

306 proliferation, recruitment or initial differentiation but is required for the expression of late-stage oligodendrocyte

307 markers during remyelination.

308

309 *Myrf deletion from OPCs leaves new oligodendrocytes prone to apoptosis*

310   Increased apoptosis occurs in the optic nerve of Myrf$^{fl/fl}$ Olig2 Cre mice during development [11] and in the

311 adult spinal cord following inducible *Myrf* deletion from mature oligodendrocytes [31]. To determine whether the

312 absence of *Myrf* increases apoptosis of oligodendrocytes following demyelination, we examined cleaved caspase-3

313 (CCasp3) expression in P-Myrf$^{fl/fl}$ and P-Myrf$^{fl/wt}$ mice (Fig. 4a, b). We found no overall difference in CCasp3+ cell

314 density between P-Myrf$^{fl/fl}$ and P-Myrf$^{fl/wt}$ mice at either 5 or 10 DPL (Fig. 4c), likely because the majority of the

315 apoptotic cells co-labelled with the pan-leukocyte marker CD45 (Fig. 4b) or the microglial/macrophage marker Iba1

11

(Fig. 4d, e). However, occasional CC1+CCasp3+ cells were observed (Fig. 4f). The density of CC1+ oligodendrocytes undergoing apoptosis was increased by approximately 4-fold at 10 DPL in P-Myrf^{fl/fl} mice (Fig. 4g). Similarly, the percentage of oligodendrocytes that were CCasp3+ was higher at 10 DPL (Fig. 4h). However, oligodendrocytes comprised the minority of apoptotic cells, even in P-Myrf^{fl/fl} mice (Fig. 4i). The truncated protein predicted to be produced in P-Myrf^{fl/fl} mice is unlikely to be directly apoptotic to oligodendrocytes as recombined oligodendrocytes persist in Myrf^{fl/fl} PLP-CreERT2 mice for weeks following *Myrf* deletion (Supplementary Fig. 2S and [31]). During remyelination, oligodendrocytes are overproduced [21], similar to developmental myelination, and compete for axonal-derived cues necessary for survival [2, 3]. New oligodendrocytes lacking *Myrf* undergo apoptosis, presumably due to impaired stabilization, ensheathment or access to axonal-derived cues. Collectively, these data suggest impairing the later stages of oligodendrocyte differentiation by deleting *Myrf* leaves oligodendrocytes vulnerable to apoptosis during remyelination.

Myrf deletion from OPCs does not induce overt demyelination, astrogliosis, or inflammation in the first two weeks following recombination

There is a continual production of new oligodendrocytes in adulthood [29, 52]. *Myrf* deletion from OPCs inhibits the formation of new oligodendrocytes during motor learning [40, 63] and could plausibly induce demyelination by impairing the differentiation of new oligodendrocytes in the healthy CNS. To determine if *Myrf* deletion resulted in demyelination in the healthy CNS during the first two weeks, we assessed myelin status by staining the uninjured side of the corpus callosum contralateral to lysolecithin injection with the myelin protein MBP (Fig. 5a, a', e, e'). We observed no overt signs of demyelination of the uninjured corpus callosum 14 DPL in P-Myrf^{fl/fl} YFP mice and GSTπ+ oligodendrocytes were readily observed (Fig. 5b, b', f, f'). Electron microscopy revealed compact myelination in both control and P-Myrf^{fl/fl} YFP mice at 14 DPL in the uninjured corpus callosum and spinal cord (Fig. 6c). Astrogliosis (Fig. 5c, c', g, g') was not observed nor clustering of microglia or obvious changes in their morphology (Fig 5d, d', h, h'), in either P-Myrf^{fl/fl} YFP or P-Myrf^{fl/wt} YFP mice. The total density of GSTπ+ oligodendrocytes (Fig. 5k) and PDGFRα+ OPCs (Fig. 5l) did not differ at 14 DPL in the contralateral non-injected corpus callosum. However, when the recombined subpopulations were examined for GSTπ (Fig. 5i) or PDGFRα (Fig. 5j), a higher percentage were found to express PDGFRα in P-Myrf^{fl/fl} YFP mice compared to P-Myrf^{fl/wt} YFP mice (Fig. 5m). Recombined cells in P-Myrf^{fl/fl} YFP mice rarely expressed GSTπ (2.41% ± 0.83%),

12

344   whereas in P-Myrf^{fl/wt} YFP mice, 15.10% ± 3.83% expressed GSTπ. Thus, *Myrf* deletion from OPCs prevents the

345   formation of new late-stage oligodendrocytes in the healthy brain as well as the demyelinated brain, but does not

346   result in overt demyelination, astrogliosis or inflammation during the first two weeks after deletion.

347

348   *MYRF is essential for remyelination*

349   *Myrf* deletion lowered the density of new GSTπ+ oligodendrocytes in response to demyelination, and as a

350   consequence should reduce the efficiency of remyelination. We examined remyelination in semithin sections of the

351   dorsal column 14 DPL in P-Myrf^{fl/fl} and P-Myrf^{fl/wt} mice (Fig. 6a). The spinal cord has larger calibre axons relative

352   to the corpus callosum allowing remyelinated axons to be easily distinguished based on their thinner myelin. This is

353   in contrast to the corpus callosum, which has many smaller axons (< 1µm) that do not always demonstrate thinner

354   myelin during remyelination [1]. In the spinal cords of control mice, numerous thinly myelinated axons, suggestive

355   of remyelination, were found (Fig. 6b, c). In contrast, there was a scarcity of thinly myelinated axons in P-Myrf^{fl/fl}

356   mice (Fig. 6b, c) that was confirmed by blinded rank analysis (Fig. 6d). We also examined the presence of MBP

357   staining in the corpus callosum to determine the extent of demyelination following lysolecithin injection in P-

358   Myrf^{fl/fl} YFP and P-Myrf^{fl/wt} YFP mice. (Fig. 6e, f). The volume of demyelination (area lacking MBP staining) did

359   not differ at 3 or 7 DPL, indicating *Myrf* deletion from OPCs did not leave the callosum more susceptible to myelin

360   loss. However, by 14 DPL there was a larger demyelinated area in P-Myrf^{fl/fl} YFP mice compared to controls (Fig.

361   6e) suggestive of impaired remyelination. Thus, in two cohorts of animals, in two different regions of the CNS,

362   MYRF was crucial for effective remyelination.

363   Remyelination can restore conductance [55], likely in part through clustering of sodium channels [18].

364   Clustering of sodium channels at nodes of Ranvier does not typically occur in the absence of oligodendrocytes and

365   myelination in the CNS [39]. To assess whether *Myrf* deletion from OPCs impaired the restoration of nodes of

366   Ranvier in lysolecithin-demyelinated lesions in the corpus callosum, we stained tissue with AnkG—to identify the

367   sodium channel scaffolding protein at the nodes—and Caspr to label paranodes. We counted nodes of Ranvier as

368   those with punctate Caspr surrounding AnkG staining (Fig. 6i) [41]. *Myrf* deletion reduced the density of nodes of

369   Ranvier within the lesion (Fig. 6g). Less axons within the lesion could also diminish node of Ranvier density, but no

370   differences in the density of SMI312+ axons were observed (Fig 6h). Thus, these data suggest a reduction of node of

371   Ranvier density is due to reduced oligodendrogenesis and not due to axon loss.

13

372   To examine axon-oligodendrocyte contact and remyelination directly in recombined cells, we crossed P-

373 Myrf^{fl/fl} and P-Myrf^{fl/wt} mice with a reporter line (mT/mG) that expressed Cre-inducible membrane-anchored GFP

374 (Fig. 7a) [42]. The membrane-anchored inducible GFP allows for the visualization of ensheathment and myelination

375 of axons by new oligodendrocytes [29]. At 28 DPL in P-Myrf^{fl/wt} mT/mG mice, OPCs were recruited to the lesion,

376 differentiated, and extended processes that co-label with MBP (Fig. 7b, d, e). In contrast, recombined cells in P-

377 Myrf^{fl/fl} mT/mG mice increased in density near the lesion but rarely co-label with MBP (Fig. 7b, d, e). There was a

378 large reduction in the capacity of recombined cells to produce myelin at 28 DPL (Fig 7c). While non-recombined

379 cells produced myelin normally in P-Myrf^{fl/fl} mT/mG mice, this was not sufficient to compensate for the recombined

380 cells and resulted in incomplete remyelination even at 28 DPL (Fig. 7c). Taking advantage of the larger axon calibre

381 in the spinal cord relative to the corpus callosum, we examined ensheathment and myelination of individual axons

382 by new oligodendrocytes in the dorsal column. While new oligodendrocytes (CC1+GFP+) were found to wrap

383 axons and produced MBP in control P-Myrf^{fl/wt} mT/mG mice following demyelination (Fig. 7f, g) new

384 oligodendrocytes in P-Myrf^{fl/fl} mT/mG mice occasionally ensheathed axons but failed to express MBP (Fig. 7f, h).

385 These data demonstrate that MYRF is required for the expression of myelin proteins in new oligodendrocytes.

386 Notably, *Myrf* deletion from OPCs does not prevent the formation of myelinating Schwann cells (P0+) from

387 recombined cells following demyelination in the spinal cord (Supplementary Fig. S6).

388

389 *MYRF expression within oligodendrocytes is correlated with successful remyelination in MS*

390   Remyelination often fails in MS [20, 46]. The expression of few transcription factors has been differentially

391 compared in human tissue between remyelinated 'shadow plaques' and chronically demyelinated lesions. Given the

392 crucial role of MYRF in rodent remyelination, we examined MYRF and the oligodendrocyte-lineage marker Sox10

393 [58, 64] in both the healthy white matter and in periventricular and subcortical white matter lesions (Fig. 8a, b).

394 MYRF was expressed in Sox10+ cells (Fig. 8c). Faint MYRF immunoreactivity was observed along blood vessels

395 or in myelin sheaths/debris. However, MYRF was not typically detected in Iba1+ microglia or GFAP+ astrocytes in

396 NAWM (Supplementary Fig. S7). In NAWM, MYRF was expressed in cells with strong NogoA expression

397 (Supplementary Fig. S8), CNP+ cells in remyelinated shadow plaques (Fig 8d), and in NogoA+ cells within the

398 active rims and centres of chronic lesions (Fig. 8e). CNP and NogoA are established markers of differentiated

14

399   oligodendrocytes in human tissue [34, 35, 50], and our data demonstrate that MYRF is expressed in

400   oligodendrocytes in the human CNS.

401   To assess whether MYRF expression is associated with remyelination in MS, we quantified the density of

402   Sox10+MYRF+ cells within lesions and NAWM. The density of both Sox10+ oligodendrocyte lineage cells and

403   Sox10+MYRF+ oligodendrocytes were reduced in the centre of chronic lesions relative to shadow plaques, chronic

404   active lesion rims and NAWM, indicating a depletion of both oligodendrocyte lineage cells and MYRF-expressing

405   oligodendrocytes within chronic lesions (Fig. 8f, g Supplementary Fig. S9). The percentage of Sox10+ cells

406   expressing MYRF was also reduced in chronic lesion centres relative to shadow plaques and NAWM (Fig. 8h). We

407   next examined NogoA, Sox10 and MYRF staining in chronic active lesions, NAWM and shadow plaques. Fewer

408   Sox10+ cells expressed strong NogoA in chronic active lesion centres relative to shadow plaques (Supplementary

409   Fig. S8 b), suggesting an accumulation of OPCs relative to oligodendrocytes. However, there was also a decreased

410   percentage of Sox10+ strongly NogoA+ oligodendrocytes expressing MYRF within chronic active lesion centres

411   relative to both chronic lesion rims, shadow plaques, and NAWM (Fig. 8i), indicating there was also a population of

412   differentiated oligodendrocytes unable to express detectable MYRF specifically in lesion centres. Collectively, the

413   increased density and capacity of oligodendrocytes to express MYRF in areas of remyelination demonstrates that

414   MYRF is associated with successful remyelination in the MS lesions examined.

415

416   **Discussion**

417   Many transcription factors crucial for developmental myelination remain poorly characterized during

418   remyelination, including MYRF. Using an inducible deletion of *Myrf* from OPCs concurrent with a focal

419   demyelinating lesion, we demonstrated that MYRF is not expressed in OPCs in the healthy or demyelinated CNS,

420   and their proliferation and recruitment to demyelinated lesions is not altered by *Myrf* deletion. However, genetic fate

421   mapping revealed that in the absence of *Myrf*, OPCs initially differentiate but are unable to robustly express late-

422   stage oligodendrocyte markers or myelin proteins. Thus, *Myrf* deletion from OPCs stalls their differentiation at the

423   premyelinating stage during remyelination (Supplementary Fig. S10). In human white matter, Sox10+NogoA+

424   oligodendrocytes were found to be positive for MYRF protein expression. We encountered fewer Sox10+MYRF+

425   cells in chronically demyelinated lesions. Additionally, a lower proportion of oligodendrocyte lineage cells

426   expressed MYRF in chronic lesion centres compared to shadow plaques or NAWM indicating a strong association

15

427   of MYRF expression with remyelination in MS. Collectively, our findings implicate MYRF in orchestrating myelin

428   regeneration in both the rodent and human CNS.

429

430   *Oligodendrocyte lineage cells in chronic MS lesions lack expression of the transcription network required for*

431   *myelination*

432   In chronic MS lesions, we find a deficiency of MYRF-expressing oligodendrocytes relative to shadow

433   plaques and NAWM. MYRF together with Sox10 constitute an essential regulatory network that drives myelin gene

434   expression [25]. The lack of MYRF expression in Sox10+ cells from chronic lesions could be a result of an

435   accumulation of OPCs relative to oligodendrocytes, supporting the notion that remyelination failure results from

436   impaired OPC differentiation [34, 61, 62]. Accordingly, we find a lower percentage of Sox10+ cells express strong

437   NogoA within chronic lesions centres relative to NAWM, suggestive of a failure to initially differentiate. However,

438   we also detect a population of Sox10+NogoA+ oligodendrocytes unable to express MYRF within chronic lesion

439   centres. NogoA is not typically expressed in OPCs [35], suggesting that these cells have differentiated but fail to

440   express MYRF and would, therefore, be unable to remyelinate. These data raise the possibility that even if OPCs are

441   able to initially differentiate, the inhibitory environment of the chronic MS lesions examined may prevent MYRF

442   expression, the later stages of differentiation, and subsequent remyelination. In mice, we demonstrated that MYRF is

443   crucial for the survival of newly generated oligodendrocytes, so an inability to express MYRF in oligodendrocytes

444   may leave them vulnerable to apoptosis. Over time, this could contribute to the severe depletion of oligodendrocytes

445   observed in most chronic MS lesions.

446   Nonetheless, in all chronic active lesions examined occasional Sox10+MYRF+ cells are found, suggesting

447   there is a population of oligodendrocytes expressing the necessary transcription factors for remyelination, yet these

448   cells are apparently unable to successfully remyelinate these lesions. This finding is in accordance with previous

449   research which indicates a population of myelin proteolipid protein expressing (PLP+) oligodendrocytes fail to

450   radially wrap axons and successfully remyelinate in the majority of chronically demyelinated lesions [7].

451   Collectively, these data imply remyelination failure in chronic lesions may be *multifactorial*. OPC differentiation

452   failure, which we define as the inability transition from a proliferative OPC to post-mitotic oligodendrocyte, along

453   with myelination failure, or the inability to wrap axons and deposit myelin, may both contribute to remyelination

454   failure. Conduction deficits in axons of chronically demyelinated lesions may inhibit effective differentiation [21]

455 and/or stabilization of oligodendrocyte wraps and subsequent myelination [24]. Additionally, inhibitory substrates

456 on axons such as polysialylated-neural cell adhesion molecule[8], myelin debris [33, 48], extracellular molecules

457 like fibronectin [57] and chondroitin sulfate proteoglycans (CSPGs) [30] may inhibit remyelination. Together these

458 and other factors could leave oligodendrocyte lineage cells in chronic MS lesions unable to express MYRF and

459 subsequently remyelinate axons.

460 Eliciting MYRF expression within oligodendrocyte lineage cells of chronic lesions may be a crucial step to

461 promote remyelination in MS. A greater understanding of the signaling pathways that induce MYRF expression

462 within premyelinating oligodendrocytes and the inhibitory influence of chronic MS lesions on these pathways will

463 be of critical importance for designing new therapeutics to overcome remyelination failure. Deletion of extracellular

464 signal–regulated kinases 1/2 (ERK1/2) in oligodendrocytes reduced the expression of *myrf* during development and

465 in the healthy CNS [27]. Conversely, sustained activation of the ERK1/2 increases *myrf* expression and reinitiates

466 myelination in quiescent oligodendrocytes in the uninjured and demyelinated CNS [28]. The antifungal agent

467 miconazole, which results in the sustained phosphorylation of ERK1/2 in OPCs, has been shown to accelerate

468 remyelination [43]. Targeting the phosphorylation of ERK1/2 with miconazole or other compounds may stimulate

469 MYRF expression and possibly overcome the inhibitory milieu of the chronic lesion and enhance remyelination.

470

471 *The Role of MYRF in Remyelination Broadly Recapitulates Developmental Myelination*

472 During both developmental myelination and remyelination, OPCs proceed through the same stages of

473 maturation from OPC to myelinating oligodendrocyte [12, 17]. This process requires the differential expression of

474 transcription factors at distinct stages of maturation [10]. We find that during remyelination, MYRF was expressed

475 with the onset of differentiation at the premyelinating stage after the downregulation of the OPC mitogen receptor

476 PDGFRα, and nearly concurrent with the expression of CC1. Given that MYRF is not expressed in OPCs during

477 remyelination, it is not surprising its deletion does not alter OPC recruitment or proliferation. Recombined cells

478 lacking MYRF can initially differentiate but have reduced expression of the more mature markers GSTπ and CNP

479 and ultimately fail to express the myelin protein MBP. Thus, during remyelination, MYRF has a unique combination

480 of characteristics amongst oligodendrocyte transcription factors; it is only expressed after initial OPC differentiation,

481 regulates the transition from premyelinating to myelinating oligodendrocyte, and is crucial for myelin gene

482 expression.

17

483   *Myrf deletion from OPCs will be a useful tool to examine the extent and mechanisms by which remyelination*

484   *protects axons*

485   Oligodendrocytes have been theorized to support axonal survival [44]. While many studies [23, 37, 45]

486   provide strong support for an essential role of oligodendrocytes in the health of axons, little *causative* evidence

487   exists that oligodendrocyte remyelination is sufficient to preserve axons during inflammatory demyelination. This is,

488   in large part, due to the difficulty of decoupling oligodendrogenesis and remyelination from inflammation and other

489   degenerative processes during demyelination. Several therapies targeting remyelination in MS are entering clinical

490   trials, and it will be crucial to determine the relative effectiveness and timeframe by which remyelination may

491   prevent axon loss following inflammatory demyelination.

492   P-Myrf$^{fl/fl}$ mice may be an excellent model to assess the sufficiency and mechanisms by remyelination

493   protects axons following demyelination. Lesions in P-Myrf$^{fl/fl}$ mice resemble those of chronic MS lesions, in that

494   these lesions contain OPCs and premyelinating oligodendrocytes, but few oligodendrocytes capable of

495   remyelinating axons. Inducible *Myrf* deletion from OPCs does not result in overt signs of demyelination, reactive

496   astrogliosis, or inflammatory lesions during the timeframe of our study, which could confound an interpretation of

497   the role of remyelination on axonal health. MYRF is also not expressed in OPCs nor alters their proliferation or

498   recruitment to areas of demyelination. Given that non-recombined cells can remyelinate normally in P-Myrf$^{fl/fl}$ mice,

499   a higher recombination efficiency of *Myrf* from OPCs would have been ideal. A second PDGFRα CreERT2 line

500   developed independently to the one used in this study has a higher recombination efficiency throughout the CNS

501   [29]. This line combined with autoimmune or cuprizone demyelination should result in long-term demyelination and

502   thus be a suitable tool to assess the efficacy, rate, and mechanisms by which new oligodendrocytes and

503   remyelination may protect axons from degeneration and enhance recovery following remyelination failure.

504   Collectively, our work demonstrates that MYRF is essential for successful remyelination by acting as a

505   master regulator crucial for the transition of oligodendrocytes from a premyelinating to myelinating phenotype. We

506   establish, for the first time, that chronic MS lesions lack oligodendrocytes that express this necessary transcription

507   factor for remyelination. Eliciting MYRF expression in oligodendrocyte lineage cells may be essential for

508   overcoming remyelination failure in MS.

509

510   **Acknowledgements**

18

519

Compliance with ethical standards

521　All animal experiments were approved by the University of British Columbia Animal Care Committee, in

522　accordance with the guidelines of the Canadian Council on Animal Care.

523

Conflict of interest

525　The authors declare that they have no competing interests.

526

538

19

Figure Legends

540 **Fig. 1** MYRF is expressed in new oligodendrocytes following focal demyelination. **a** Schematic of the transgenic

541 mice used, lysolecithin injection location and experimental timeline. **b** Micrographs of MYRF and YFP expression

542 in demyelinating lesions at 3, 7 and 14 DPL in P-Myrf$^{fl/wt}$ YFP mice. Dashed line demarcates the approximate lesion

543 boundary. **c** Quantification of MYRF+ cell density demonstrates increased density in P-Myrf$^{fl/wt}$ YFP mice between

544 3 and 7 DPL *(P=0.013)* and 3 and 14 DPL (P<0.001). **d** Quantification indicating an increase in the percentage of

545 recombined cells (YFP+) which are also MYRF+ by 7 DPL (P=0.001) and 14 DPL (P<0.001) relative to 3 DPL. **e**

546 Micrographs demonstrating that some recombined cells have differentiated and express the mature oligodendrocyte

547 marker CC1, which often co-label with MYRF (arrowheads) in P-Myrf$^{fl/wt}$ YFP mice 7 DPL. In P-Myrf$^{fl/fl}$ YFP

548 mice, many recombined cells have either faint or undetectable expression of MYRF in newly differentiated

549 oligodendrocytes (arrows). **f** Micrograph indicating MYRF is not expressed in PDGFRα+ cells in lesions or adjacent

550 to lesion boundaries (dashed line). **g** Quantification demonstrating the percentage of recombined oligodendrocytes

551 (CC1+YFP+) that express MYRF is reduced at 7 DPL *(P<0.001),* and 14 DPL *(P=0.016)* in P-Myrf$^{fl/fl}$ YFP relative

552 to P-Myrf$^{fl/wt}$ YFP mice. **h** Quantification using primers specific for recombined *myrf* (lacking exon 8) shows there

553 is an increase in expression within the brain of P-Myrf$^{fl/fl}$ mice treated with tamoxifen *(P=0.036)* compared to P-

554 Myrf$^{fl/fl}$ mice that did not receive tamoxifen. Two-way ANOVA followed by Tukey's *post hoc* test in **c**, **g** and

555 Tamhane's *post hoc* test in **d**. *n*=4-6 mice per group per timepoint in **c**, **d** and **g**. Kruskal-Wallis test followed by

556 Dunn's test, *n*=3-4 per group in **h**. Scale bars are 50 µm in **b** and 20µm in **e** and **f**

557 **Fig. 2** MYRF is not required for OPC recruitment or proliferation in demyelinated lesions. **a** Representative

558 photomicrographs of lesion epicentre stained for CNP and Ki67 or YFP and PDGFRα in P-Myrf$^{fl/wt}$ YFP and P-

559 Myrf$^{fl/fl}$ YFP mice 3 DPL. Dashed line demarcates approximate lesion boundary. **b** Quantification of PDGFRα+ cell

560 density indicates there is no difference between P-Myrf$^{fl/fl}$ YFP and P-Myrf$^{fl/wt}$ YFP mice at any time point. **c**

561 Quantification demonstrating Ki67+PDGFRα+ cell density does not differ between P-Myrf$^{fl/wt}$ YFP and P-Myrf$^{fl/fl}$

562 YFP mice at 3, 7 or 14 DPL, but declines between 3 DPL and 7 DPL in both groups *(P-Myrf$^{fl/wt}$ YFP P<0.001, P-*

563 *Myrf$^{fl/fl}$ YFP P=0.002)*. **d** Single optical confocal section demonstrating co-labelling between YFP, PDGFRα, and

564 Ki67 (arrowheads) in P-Myrf$^{fl/wt}$ YFP and **e** P-Myrf$^{fl/fl}$ YFP mice. Arrows indicate YFP+PDGFRα+Ki67- cells. **f**

565 Quantification indicating the percentage of PDGFRα+ cells which express Ki67 does not differ between P-Myrf$^{fl/fl}$

566 and P-Myrf$^{fl/wt}$ mice at any time point, but declines between 3 and 7 DPL in both P-Myrf$^{fl/wt}$ YFP (*P<0.001*) and P-

567 Myrf$^{fl/fl}$ YFP (*P<0.001*) mice. **g** Quantification demonstrating the percentage of recombined OPCs

568 (YFP+PDGFRα+) that are Ki67+ does not differ between P-Myrf$^{fl/wt}$ YFP and P-Myrf$^{fl/fl}$ YFP mice at any time point

569 examined but declines between 3 and 7 DPL in both P-Myrf$^{fl/wt}$ YFP (*P<0.001*) and P-Myrf$^{fl/fl}$ YFP (*P<0.001*) mice.

570 Scale bars are 50µm in **a** and 10µm in **d**, and **e**. Two-way ANOVA followed by Tukey's *post hoc* test for **b**, **c**, **f**, **g**.

571 *n*=4-6 mice per group per timepoint.

572 **Fig. 3** *Myrf* deletion does not alter the transition from an OPC to premyelinating oligodendrocyte, but inhibits the

573 later stages of oligodendrocyte differentiation during remyelination. **a** Photomicrographs of a single optical confocal

574 section of the lesion at 7 DPL. Recombined cells within lesions express either CC1 (arrowheads) or PDGFRα

575 (arrows), in both P-Myrf$^{fl/wt}$ YFP and P-Myrf$^{fl/fl}$ YFP mice. **b** Quantification demonstrating the percentage of

576 recombined cells that are CC1+does not differ at any time point examined between P-Myrf$^{fl/wt}$ YFP and P-Myrf$^{fl/fl}$

577 YFP mice but increases in both groups between 3 and 14 DPL (*P-Myrf$^{fl/wt}$ YFP P<0.001, P-Myrf$^{fl/fl}$ YFP P<0.001*). **c**

578 Quantification of demonstrating the percentage of recombined cells that are PDGFRα+ does not differ between P-

579 Myrf$^{fl/wt}$ YFP and P-Myrf$^{fl/fl}$ YFP mice at any time point examined; but the percentage of cells declines in both

580 groups between 3 and 14 DPL (*P-Myrf$^{fl/wt}$ YFP P=0.003, P-Myrf$^{fl/fl}$ YFP P=0.002*). **d** Representative

581 photomicrograph of lesion epicentre 14 DPL in both P-Myrf$^{fl/wt}$ YFP and P-Myrf$^{fl/fl}$ YFP mice stained for YFP,

582 GSTπ and CNP. Dashed lines demarcate lesion boundaries. **e** Single optical section demonstrating considerable co-

583 labelling between YFP, GSTπ (arrowheads) and CNP in P-Myrf$^{fl/wt}$ YFP mice 14 DPL. **f** Recombined cells in P-

584 Myrf$^{fl/fl}$ YFP mice rarely express GSTπ. **g** Quantification demonstrating that the percentage of recombined cells that

585 are CNP+ (*P=0.021*) and **h** GSTπ+ (*P<0.001*) declines in P-Myrf$^{fl/fl}$ YFP compared to P-Myrf$^{fl/wt}$ YFP mice at 14

586 DPL **i** Quantification indicating the total GSTπ+ cell density is reduced within the lesion at 14 DPL in P-Myrf$^{f/fl}$

587 YFP compared to P-Myrf$^{fl/wt}$ YFP mice (*P=0.043*). All statistical comparisons in **b**, **c**, **g**, **h**, **i** used a two-way

588 ANOVA followed by Tukey's *post hoc* test, *n*=4-6 mice per group per timepoint. Scale bars are 20µm in **a**, **e** and **f**

589 and 50µm in **d**

590 **Fig. 4** Oligodendrocytes are more prone to apoptosis following *Myrf* deletion from OPCs during remyelination. **a**

591 Representative photomicrographs of demyelinated lesion stained for MBP and CCasp3 at 5 and 10 DPL in both P-

592 Myrf$^{fl/wt}$ and P-Myrf$^{fl/fl}$ mice. Dashed line demarcates approximate lesion boundary. **b** Micrograph of the lesion

21

593   epicentre stained with CD45 and CCasp3 in P-Myrf$^{fl/wt}$ and P-Myrf$^{fl/fl}$ mice at 10 DPL. The majority of CCasp3+

594   cells associate with CD45. **c** Quantification of total CCasp3+Hoechst+ (apoptotic) cell density. **d** Single optical

595   confocal section demonstrating that CCasp3+ is expressed in CD45+ cells (arrowhead), and many cells also express

596   the microglia/macrophage marker Iba1 in both P-Myrf$^{fl/wt}$ and **e** P-Myrf$^{fl/fl}$ mice. **f** Single optical confocal section at

597   10 DPL in P-Myrf$^{fl/fl}$ mice, with single channels of Hoechst, CC1 and CCasp3. Arrowhead indicates

598   CC1+Hoechst+CCasp3+ cell. **g** Quantification indicating CC1+CCasp3+ density is higher in P-Myrf$^{fl/fl}$ compared to

599   P-Myrf$^{fl/wt}$ mice at 10 DPL (*P=0.039*). **h** Quantification demonstrating increased percentage of CC1+ cells are

600   CCasp3+ in P-Myrf$^{fl/fl}$ compared to P-Myrf$^{fl/wt}$ mice at 10 DPL (*P=0.028*). **i** Quantification revealing an increase at

601   10 DPL in the percentage of apoptotic cells that express CC1 in P-Myrf$^{fl/fl}$ relative to P-Myrf$^{fl/wt}$ mice (*P=0.028*).

602   Two-way ANOVA followed by Tukey's *post hoc* test to determine individual group differences for **c**, **g**, **h** and **i**.

603   *n*=4-5 mice per group per timepoint. Scale bars are 50µm in **a**, 20 µm in **b** and 5 µm in **d**, **e**, and **f**

604   **Fig. 5** *Myrf* deletion from OPCs does not induce overt demyelination, astrogliosis or inflammation but reduces the

605   number of new oligodendroctyes in the healthy brain two weeks following tamoxifen injection. P-Myrf$^{fl/wt}$ YFP and

606   P-Myrf$^{fl/fl}$ YFP mice were examined on the contralateral side of the corpus callosum (CC) to the lysolecithin lesion

607   14 DPL. Representative photomicrographs of staining with **a, a'** MBP, **b, b'** GSTπ, **c, c'** GFAP and **d, d'** Iba1.

608   Enlarged images of **e, e'** MBP, **f, f'** GSTπ, **g, g'** GFAP and **h, h'** Iba1. **i** Single merged confocal optical section in

609   the corpus callosum contralateral to lysolecithin lesion in P-Myrf$^{fl/wt}$ mice 14 DPL demonstrating occasional

610   YFP+GSTπ+ oligodendrocytes (arrowhead). Single channel micrograph showing **i'** YFP and **i"** GSTπ. **j** Single

611   merged optical section in the corpus callosum contralateral to the lysolecithin lesion of P-Myrf$^{fl/wt}$ mice 14 DPL

612   demonstrating co-labelling between YFP and PDGFRα (arrowheads). Arrows indicate PDGFRα+ cells which did

613   not recombine (YFP-). Single channel image showing **j'** YFP and **j"** PDGFRα. Quantification showing no

614   difference in cell density of **k** (GSTπ+) and **l** (PDGFRα+) cells in the contralateral side of the corpus callosum

615   between P-Myrf$^{fl/wt}$ and P-Myrf$^{fl/fl}$ mice. **m** Quantification demonstrating recombined cells are unable to differentiate

616   into CNP+ (*P=0.027*) or GSTπ+ (*P=0.032*) oligodendrocytes and a greater percentage remain PDGFRα+ (*P=0.016*)

617   in P-Myrf$^{fl/fl}$ YFP relative to P-Myrf$^{fl/wt}$ YFP mice. Student's T-Test in **k** and **l** and Mann Whitney U Test in **m**, *n*=4-

618   5 mice per group. Scale bars are 100µm in (**a-d**) and (**a'-d'**) and 20µm in (**e-h**),(**e'-h'**), **i**, **i'**, **i"** and **j**, **j'**, **j"**

22

619 **Fig. 6** *Myrf* deletion from OPCs inhibits remyelination. **a** Schematic demonstrating the location of lysolecithin

620 injections into the dorsal column of the C4 spinal cord and location of semi-thin and electron micrographs. **b**

621 Semithin sections at the C4 spinal cord level stained with toluidine blue from P-Myrf[fl/wt] and P-Myrf^{fl/fl} mice. There

622 are few myelinated axons in P-Myrf^{fl/fl} mice. **c** Electron micrographs of the uninjured and 14 DPL C4 spinal cord in

623 P-Myrf[fl/wt] and P-Myrf^{fl/fl} mice. **d** Ranking analysis in P-Myrf^{fl/fl} and P-Myrf[fl/wt] mice, demonstrates there is less

624 remyelination in P-Myrf^{fl/fl} mice (*P=0.030).* **e** Quantification of the volume of spared tissue that is MBP-negative

625 within the corpus callosum. At 14 DPL, there is a reduction in the MBP-negative volume in P-Myrf[fl/wt] YFP relative

626 to P-Myrf^{fl/fl} YFP mice (P=0.028). **f** Overview of lesion epicentre in the corpus callosum stained with MBP at 3, 7,

627 and 14 DPL in P-Myrf[fl/wt] YFP and P-Myrf^{fl/fl} YFP mice. MBP is expressed throughout the corpus callosum at 14

628 DPL in P-Myrf[fl/wt] YFP in contrast to P-Myrf^{fl/fl} YFP mice. **g** Quantifications indicating node of Ranvier density in

629 the corpus callosum is reduced (*P=0.047*) but **h** SMI312+ axon staining does not differ between P-Myrf[fl/wt] YFP and

630 P-Myrf^{fl/fl} YFP mice at 14 DPL (*P=0.754*) in the corpus callosum. **i** Example micrograph of a subset of lesion

631 demonstrating notably fewer punctate Caspr flanking AnkG, in P-Myrf^{fl/fl} YFP relative to P-Myrf[fl/wt] YFP mice at 14

632 DPL. Mann Whitney U Test used in **d**, **e** and **g**, Student's T-test in **h**. *n*=4-6 mice per group per time point. Scale

633 bars are 50µm in **b** and **f**, 20µm **i** and 2 µm in **c**

634 **Fig. 7** New oligodendrocytes are unable to effectively remyelinate in P-Myrf^{fl/fl} mT/mG mice. **a** Schematic of the

635 transgenic lines used and experimental timeline. All mice were perfused 28 DPL. **b** Overview of lysolecithin lesion

636 in the corpus callosum stained for GFP and MBP in P-Myrf[fl/wt] mT/mG and P-Myrf^{fl/fl} mT/mG mice. **c**

637 Quantification demonstrating reductions in the amount of myelin generated by recombined cells within the lesion

638 (GFP+MBP+) in P-Myrf^{fl/fl} mT/mG relative to P-Myrf[fl/wt] mice (green bars, Mann Whitney U test, *P=0.006*) but

639 myelin generated by non-recombined cells (GFP-MBP+) does not change (clear portion of bars, T-Test, P=0.236).

640 There is less overall MBP in P-Myrf^{fl/fl} mT/mG mice in the lesion (total of bars, T-Test, P=0.020). *n*=6 mice per

641 group. **d** Single optical section of the corpus callosum with axons in cross section reveals co-labelling of GFP with

642 MBP in P-Myrf[fl/wt] mT/mG mice but almost no GFP+MBP+ sheaths in P-Myrf^{fl/fl} mT/mG mice. **e** Processes from

643 CC1+GFP+ oligodendrocytes (arrowheads) are seen to align along myelinated fibers and co-label with MBP

644 (yellow) in P-Myrf[fl/wt] mT/mG mice adjacent to lesion epicentre but CC1+GFP+ cells rarely have processes which

645 co-label with MBP in P-Myrf^{fl/fl} mT/mG mice. **f** Single optical confocal coronal section taken at the C4 level of the

646 spinal cord of P-Myrf[fl/wt] mT/mG and P-Myrf^{fl/fl} mT/mG mice stained with SMI312, MBP, GFP and CC1. Arrows

23

647 indicate GFP+CC1+ cell bodies. **g** Enlarged image of individual oligodendrocyte processes from P-Myrf[fl/wt] mT/mG

648 mice. Within the lesion, numerous GFP+ process surround axons and co-label with MBP indicative of new

649 myelination. **h** Occasional GFP+CC1+ oligodendrocytes wrap axons in P-Myrf^{fl/fl} mT/mG mice, but rarely express

650 MBP. In **g** and **h** arrowheads demarcate GFP+MBP+ myelin, and arrows indicate GFP+ processes wrapping axons

651 that are MBP-negative. Scale bars are 50µm in **b**,10 µm in **d, e** and **f** and 5µm in **g** and **h**

652 **Fig 8** Successful remyelination in MS lesions is associated with MYRF expression in oligodendrocytes. **a**

653 Micrographs of human MS lesions and NAWM stained with luxol fast blue (LFB). Demyelination is observed in

654 active and chronic active plaques, whereas faint LFB staining is present in shadow plaques. **b** Class II HLA

655 reactivity is perilesional in chronic active plaques, and found throughout the lesion in active plaques. **c** Co-labelling

656 between MYRF and the oligodendrocyte lineage marker Sox10 is seen in NAWM. MYRF is primarily nuclear, as

657 indicated by co-labelling with Hoechst. **d** Single optical confocal section demonstrating MYRF is expressed in

658 CNP+ cells within shadow plaques (arrowheads). Arrows indicate CNP+MYRF-negative cells. **e** Example

659 micrographs of single optical confocal sections in chronic active lesion centres and rims demonstrating MYRF is

660 typically expressed in Sox10+NogoA+ oligodendrocytes (arrowhead). Arrows denote Sox10+NogoA+ cells which

661 lack MYRF. **f** Less Hoechst+Sox10+ cells are observed in the centre of chronic active lesions relative to active

662 lesions (*P=0.042*), chronic active rim (*P<0.001*), shadow plaques (*P=0.026*), NAWM (*P<0.001*), and non-MS

663 (*P<0.001*). **g** Less Hoechst+Sox10+MYRF+ cells in chronic lesion centres compared to all other groups (*active*

664 *lesions P=0.016, chronic active rim P=0.002, shadow plaques P=0.012, NAWM P<0.001, and non-MS P<0.001*). **h**

665 The percentage of Hoechst+Sox10+ cells that express MYRF is reduced in chronic active lesions relative to shadow

666 plaques (*P=0.041*), NAWM (*P<0.001*) and non-MS white matter (*P<0.001*). **i** The percentage of Sox10+NogoA+

667 oligodendrocytes which express MYRF is reduced in chronic active lesion centres relative to NAWM (*P<0.001*),

668 shadow plaques (*P<0.001*), and chronic active rims (*P<0.001*). Horizontal lines with vertical dashes above

669 quantifications in **f-i** indicate all statistically significant *post hoc* tests relative to the group with the larger vertical

670 line. One-way ANOVA followed by Tukey's *post hoc* for **f, g, h, i**. Scale bars are 500 µm in **a** and **b**, 50µm in **c**,

671 20µm in **d** and 10µm in **e**. * = statistical significance

672

673 **References**

24

674   1   Bai CB, Sun S, Roholt A, Benson E, Edberg D, Medicetty S, et al. (2016) A mouse model for testing
675   remyelinating therapies. Exp Neurol 283: 330-340 Doi 10.1016/j.expneurol.2016.06.033

676   2   Barres BA, Raff MC (1999) Axonal control of oligodendrocyte development. The Journal of cell
677   biology 147: 1123-1128

678   3   Barres BA, Raff MC (1994) Control of Oligodendrocyte Number in the Developing Rat Optic-
679   Nerve. Neuron 12: 935-942 Doi 10.1016/0896-6273(94)90305-0

680   4   Bo L, Mork S, Kong PA, Nyland H, Pardo CA, Trapp BD (1994) Detection of MHC class II-antigens
681   on macrophages and microglia, but not on astrocytes and endothelia in active multiple sclerosis
682   lesions. Journal of neuroimmunology 51: 135-146

683   5   Bujalka H, Koenning M, Jackson S, Perreau VM, Pope B, Hay CM, et al. (2013) MYRF Is a
684   Membrane-Associated Transcription Factor That Autoproteolytically Cleaves to Directly Activate
685   Myelin Genes. PLoS biology 11: Doi 10.1371/journal.pbio.1001625

686   6   Cahoy JD, Emery B, Kaushal A, Foo LC, Zamanian JL, Christopherson KS, et al. (2008) A
687   transcriptome database for astrocytes, neurons, and oligodendrocytes: a new resource for
688   understanding brain development and function. J Neurosci 28: 264-278 Doi
689   10.1523/JNEUROSCI.4178-07.2008

690   7   Chang A, Tourtellotte WW, Rudick R, Trapp BD (2002) Premyelinating oligodendrocytes in
691   chronic lesions of multiple sclerosis. The New England journal of medicine 346: 165-173 Doi
692   10.1056/NEJMoa010994

693   8   Charles P, Hernandez MP, Stankoff B, Aigrot MS, Colin C, Rougon G, et al. (2000) Negative
694   regulation of central nervous system myelination by polysialylated-neural cell adhesion
695   molecule. Proc Natl Acad Sci U S A 97: 7585-7590 Doi 10.1073/pnas.100076197

696   9   Denk F, Ramer LM, Erskine EL, Nassar MA, Bogdanov Y, Signore M, et al. (2015) Tamoxifen
697   induces cellular stress in the nervous system by inhibiting cholesterol synthesis. Acta
698   neuropathologica communications 3: 74 Doi 10.1186/s40478-015-0255-6

699   10   Emery B (2010) Transcriptional and post-transcriptional control of CNS myelination. Current
700   opinion in neurobiology 20: 601-607 Doi 10.1016/j.conb.2010.05.005

701   11   Emery B, Agalliu D, Cahoy JD, Watkins TA, Dugas JC, Mulinyawe SB, et al. (2009) Myelin gene
702   regulatory factor is a critical transcriptional regulator required for CNS myelination. Cell 138:
703   172-185 Doi 10.1016/j.cell.2009.04.031

704   12   Fancy SP, Chan JR, Baranzini SE, Franklin RJ, Rowitch DH (2011) Myelin regeneration: a
705   recapitulation of development? Annu Rev Neurosci 34: 21-43 Doi 10.1146/annurev-neuro-
706   061010-113629

707   13   Fancy SP, Harrington EP, Yuen TJ, Silbereis JC, Zhao C, Baranzini SE, et al. (2011) Axin2 as
708   regulatory and therapeutic target in newborn brain injury and remyelination. Nat Neurosci 14:
709   1009-1016 Doi 10.1038/nn.2855

710   14   Fancy SP, Kotter MR, Harrington EP, Huang JK, Zhao C, Rowitch DH, et al. (2010) Overcoming
711   remyelination failure in multiple sclerosis and other myelin disorders. Exp Neurol 225: 18-23 Doi
712   10.1016/j.expneurol.2009.12.020

713   15   Franklin RJ, Ffrench-Constant C (2008) Remyelination in the CNS: from biology to therapy. Nat
714   Rev Neurosci 9: 839-855 Doi 10.1038/nrn2480

715   16   Franklin RJ, ffrench-Constant C, Edgar JM, Smith KJ (2012) Neuroprotection and repair in
716   multiple sclerosis. Nature reviews Neurology 8: 624-634 Doi 10.1038/nrneurol.2012.200

717   17   Franklin RJ, Hinks GL (1999) Understanding CNS remyelination: clues from developmental and
718   regeneration biology. Journal of neuroscience research 58: 207-213

719   18   Freeman SA, Desmazieres A, Simonnet J, Gatta M, Pfeiffer F, Aigrot MS, et al. (2015)
720   Acceleration of conduction velocity linked to clustering of nodal components precedes
721   myelination. Proc Natl Acad Sci U S A 112: E321-328 Doi 10.1073/pnas.1419099112

25

19   Frischer JM, Bramow S, Dal-Bianco A, Lucchinetti CF, Rauschka H, Schmidbauer M, et al. (2009) The relation between inflammation and neurodegeneration in multiple sclerosis brains. Brain 132: 1175-1189 Doi 10.1093/brain/awp070

20   Frischer JM, Weigand SD, Guo Y, Kale N, Parisi JE, Pirko I, et al. (2015) Clinical and pathological insights into the dynamic nature of the white matter multiple sclerosis plaque. Annals of neurology 78: 710-721 Doi 10.1002/ana.24497

21   Gautier HO, Evans KA, Volbracht K, James R, Sitnikov S, Lundgaard I, et al. (2015) Neuronal activity regulates remyelination via glutamate signalling to oligodendrocyte progenitors. Nat Commun 6: 8518 Doi 10.1038/ncomms9518

22   Gonzalez GA, Hofer MP, Syed YA, Amaral AI, Rundle J, Rahman S, et al. (2016) Tamoxifen accelerates the repair of demyelinated lesions in the central nervous system. Sci Rep 6: 31599 Doi 10.1038/srep31599

23   Griffiths I, Klugmann M, Anderson T, Yool D, Thomson C, Schwab MH, et al. (1998) Axonal swellings and degeneration in mice lacking the major proteolipid of myelin. Science 280: 1610-1613

24   Hines JH, Ravanelli AM, Schwindt R, Scott EK, Appel B (2015) Neuronal activity biases axon selection for myelination in vivo. Nat Neurosci 18: 683-689 Doi 10.1038/nn.3992

25   Hornig J, Frob F, Vogl MR, Hermans-Borgmeyer I, Tamm ER, Wegner M (2013) The transcription factors Sox10 and Myrf define an essential regulatory network module in differentiating oligodendrocytes. PLoS genetics 9: e1003907 Doi 10.1371/journal.pgen.1003907

26   Irvine KA, Blakemore WF (2008) Remyelination protects axons from demyelination-associated axon degeneration. Brain 131: 1464-1477 Doi 10.1093/brain/awn080

27   Ishii A, Furusho M, Dupree JL, Bansal R (2014) Role of ERK1/2 MAPK signaling in the maintenance of myelin and axonal integrity in the adult CNS. J Neurosci 34: 16031-16045 Doi 10.1523/JNEUROSCI.3360-14.2014

28   Jeffries MA, Urbanek K, Torres L, Wendell SG, Rubio ME, Fyffe-Maricich SL (2016) ERK1/2 Activation in Preexisting Oligodendrocytes of Adult Mice Drives New Myelin Synthesis and Enhanced CNS Function. J Neurosci 36: 9186-9200 Doi 10.1523/JNEUROSCI.1444-16.2016

29   Kang SH, Fukaya M, Yang JK, Rothstein JD, Bergles DE (2010) NG2+ CNS glial progenitors remain committed to the oligodendrocyte lineage in postnatal life and following neurodegeneration. Neuron 68: 668-681 Doi 10.1016/j.neuron.2010.09.009

30   Keough MB, Rogers JA, Zhang P, Jensen SK, Stephenson EL, Chen T, et al. (2016) An inhibitor of chondroitin sulfate proteoglycan synthesis promotes central nervous system remyelination. Nat Commun 7: 11312 Doi 10.1038/ncomms11312

31   Koenning M, Jackson S, Hay CM, Faux C, Kilpatrick TJ, Willingham M, et al. (2012) Myelin gene regulatory factor is required for maintenance of myelin and mature oligodendrocyte identity in the adult CNS. J Neurosci 32: 12528-12542 Doi 10.1523/JNEUROSCI.1069-12.2012

32   Kornek B, Storch MK, Weissert R, Wallstroem E, Stefferl A, Olsson T, et al. (2000) Multiple sclerosis and chronic autoimmune encephalomyelitis: a comparative quantitative study of axonal injury in active, inactive, and remyelinated lesions. Am J Pathol 157: 267-276 Doi 10.1016/S0002-9440(10)64537-3

33   Kotter MR, Li WW, Zhao C, Franklin RJ (2006) Myelin impairs CNS remyelination by inhibiting oligodendrocyte precursor cell differentiation. J Neurosci 26: 328-332 Doi 10.1523/JNEUROSCI.2615-05.2006

34   Kuhlmann T, Miron V, Cuo Q, Wegner C, Antel J, Bruck W (2008) Differentiation block of oligodendroglial progenitor cells as a cause for remyelination failure in chronic multiple sclerosis. Brain 131: 1749-1758 Doi 10.1093/brain/awn096

26

769   35   Kuhlmann T, Remington L, Maruschak B, Owens T, Bruck W (2007) Nogo-A is a reliable
770   oligodendroglial marker in adult human and mouse CNS and in demyelinated lesions. J
771   Neuropath Exp Neur 66: 238-246

772   36   Kutzelnigg A, Lucchinetti CF, Stadelmann C, Bruck W, Rauschka H, Bergmann M, et al. (2005)
773   Cortical demyelination and diffuse white matter injury in multiple sclerosis. Brain 128: 2705-
774   2712 Doi 10.1093/brain/awh641

775   37   Lappe-Siefke C, Goebbels S, Gravel M, Nicksch E, Lee J, Braun PE, et al. (2003) Disruption of Cnp1
776   uncouples oligodendroglial functions in axonal support and myelination. Nature genetics 33:
777   366-374 Doi 10.1038/ng1095

778   38   Livak KJ, Schmittgen TD (2001) Analysis of relative gene expression data using real-time
779   quantitative PCR and the 2(T)(-Delta Delta C) method. Methods 25: 402-408 Doi
780   10.1006/meth.2001.1262

781   39   Mathis C, Denisenko-Nehrbass N, Girault JA, Borrelli E (2001) Essential role of oligodendrocytes
782   in the formation and maintenance of central nervous system nodal regions. Development 128:
783   4881-4890

784   40   McKenzie IA, Ohayon D, Li H, de Faria JP, Emery B, Tohyama K, et al. (2014) Motor skill learning
785   requires active central myelination. Science 346: 318-322 Doi 10.1126/science.1254960

786   41   Miron VE, Boyd A, Zhao JW, Yuen TJ, Ruckh JM, Shadrach JL, et al. (2013) M2 microglia and
787   macrophages drive oligodendrocyte differentiation during CNS remyelination. Nat Neurosci 16:
788   1211-1218 Doi 10.1038/nn.3469

789   42   Muzumdar MD, Tasic B, Miyamichi K, Li L, Luo L (2007) A global double-fluorescent Cre reporter
790   mouse. Genesis 45: 593-605 Doi 10.1002/dvg.20335

791   43   Najm FJ, Madhavan M, Zaremba A, Shick E, Karl RT, Factor DC, et al. (2015) Drug-based
792   modulation of endogenous stem cells promotes functional remyelination in vivo. Nature 522:
793   216-220 Doi 10.1038/nature14335

794   44   Nave KA (2010) Myelination and support of axonal integrity by glia. Nature 468: 244-252 Doi
795   10.1038/nature09614

796   45   Nguyen T, Mehta NR, Conant K, Kim KJ, Jones M, Calabresi PA, et al. (2009) Axonal protective
797   effects of the myelin-associated glycoprotein. J Neurosci 29: 630-637 Doi
798   10.1523/JNEUROSCI.5204-08.2009

799   46   Patrikios P, Stadelmann C, Kutzelnigg A, Rauschka H, Schmidbauer M, Laursen H, et al. (2006)
800   Remyelination is extensive in a subset of multiple sclerosis patients. Brain 129: 3165-3172 Doi
801   10.1093/Brain/Awl217

802   47   Piaton G, Aigrot MS, Williams A, Moyon S, Tepavcevic V, Moutkine I, et al. (2011) Class 3
803   semaphorins influence oligodendrocyte precursor recruitment and remyelination in adult
804   central nervous system. Brain 134: 1156-1167 Doi 10.1093/brain/awr022

805   48   Plemel JR, Manesh SB, Sparling JS, Tetzlaff W (2013) Myelin inhibits oligodendroglial maturation
806   and regulates oligodendrocytic transcription factor expression. Glia 61: 1471-1487 Doi
807   10.1002/Glia.22535

808   49   Prineas JW, Barnard RO, Kwon EE, Sharer LR, Cho ES (1993) Multiple sclerosis: remyelination of
809   nascent lesions. Annals of neurology 33: 137-151 Doi 10.1002/ana.410330203

810   50   Prineas JW, Kwon EE, Goldenberg PZ, Ilyas AA, Quarles RH, Benjamins JA, et al. (1989) Multiple
811   sclerosis. Oligodendrocyte proliferation and differentiation in fresh lesions. Laboratory
812   investigation; a journal of technical methods and pathology 61: 489-503

813   51   Raine CS, Wu E (1993) Multiple sclerosis: remyelination in acute lesions. J Neuropathol Exp
814   Neurol 52: 199-204

27

815 52 Rivers LE, Young KM, Rizzi M, Jamen F, Psachoulia K, Wade A, et al. (2008) PDGFRA/NG2 glia
816 generate myelinating oligodendrocytes and piriform projection neurons in adult mice. Nat
817 Neurosci 11: 1392-1401 Doi 10.1038/nn.2220
818 53 Schneider S, Gruart A, Grade S, Zhang Y, Kroger S, Kirchhoff F, et al. (2016) Decrease in newly
819 generated oligodendrocytes leads to motor dysfunctions and changed myelin structures that
820 can be rescued by transplanted cells. Glia 64: 2201-2218 Doi 10.1002/glia.23055
821 54 Scholzen T, Gerdes J (2000) The Ki-67 protein: from the known and the unknown. Journal of
822 cellular physiology 182: 311-322 Doi 10.1002/(SICI)1097-4652(200003)182:3<311::AID-
823 JCP1>3.0.CO;2-9
824 55 Smith KJ, Blakemore WF, Mcdonald WI (1979) Central Remyelination Restores Secure
825 Conduction. Nature 280: 395-396 Doi 10.1038/280395a0
826 56 Srinivas S, Watanabe T, Lin CS, William CM, Tanabe Y, Jessell TM, et al. (2001) Cre reporter
827 strains produced by targeted insertion of EYFP and ECFP into the ROSA26 locus. BMC
828 developmental biology 1: 4 Doi 10.1186/1471-213X-1-4
829 57 Stoffels JM, de Jonge JC, Stancic M, Nomden A, van Strien ME, Ma D, et al. (2013) Fibronectin
830 aggregation in multiple sclerosis lesions impairs remyelination. Brain 136: 116-131 Doi
831 10.1093/brain/aws313
832 58 Stolt CC, Rehberg S, Ader M, Lommes P, Riethmacher D, Schachner M, et al. (2002) Terminal
833 differentiation of myelin-forming oligodendrocytes depends on the transcription factor Sox10.
834 Genes & development 16: 165-170 Doi 10.1101/gad.215802
835 59 van der Valk P, De Groot CJ (2000) Staging of multiple sclerosis (MS) lesions: pathology of the
836 time frame of MS. Neuropathology and applied neurobiology 26: 2-10
837 60 Wingerchuk DM, Weinshenker BG (2000) Multiple sclerosis: epidemiology, genetics,
838 classification, natural history, and clinical outcome measures. Neuroimaging Clin N Am 10: 611-
839 624 ,vii
840 61 Wolswijk G (2002) Oligodendrocyte precursor cells in the demyelinated multiple sclerosis spinal
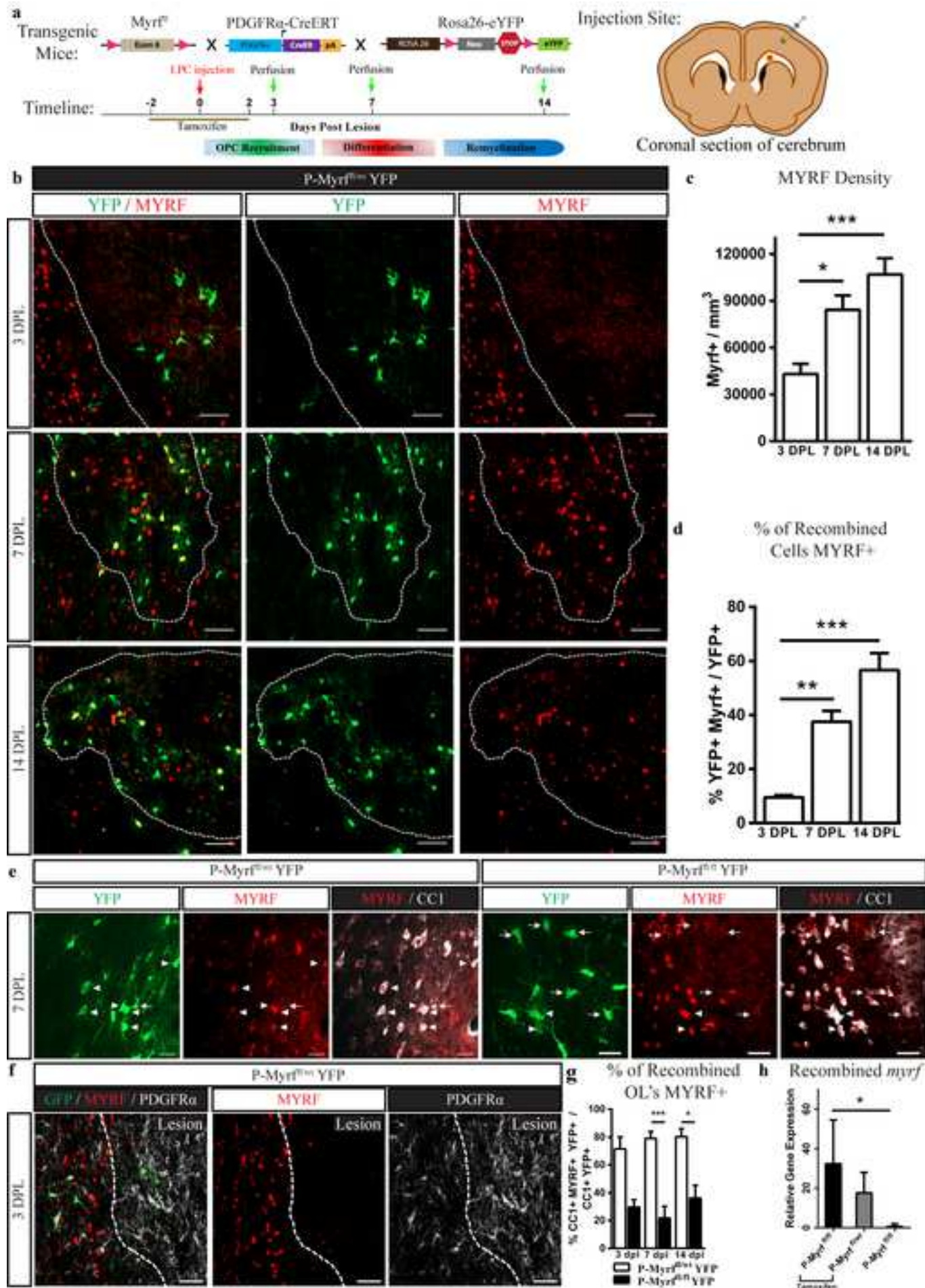841 cord. Brain 125: 338-349
842 62 Wolswijk G (2000) Oligodendrocyte survival, loss and birth in lesions of chronic-stage multiple
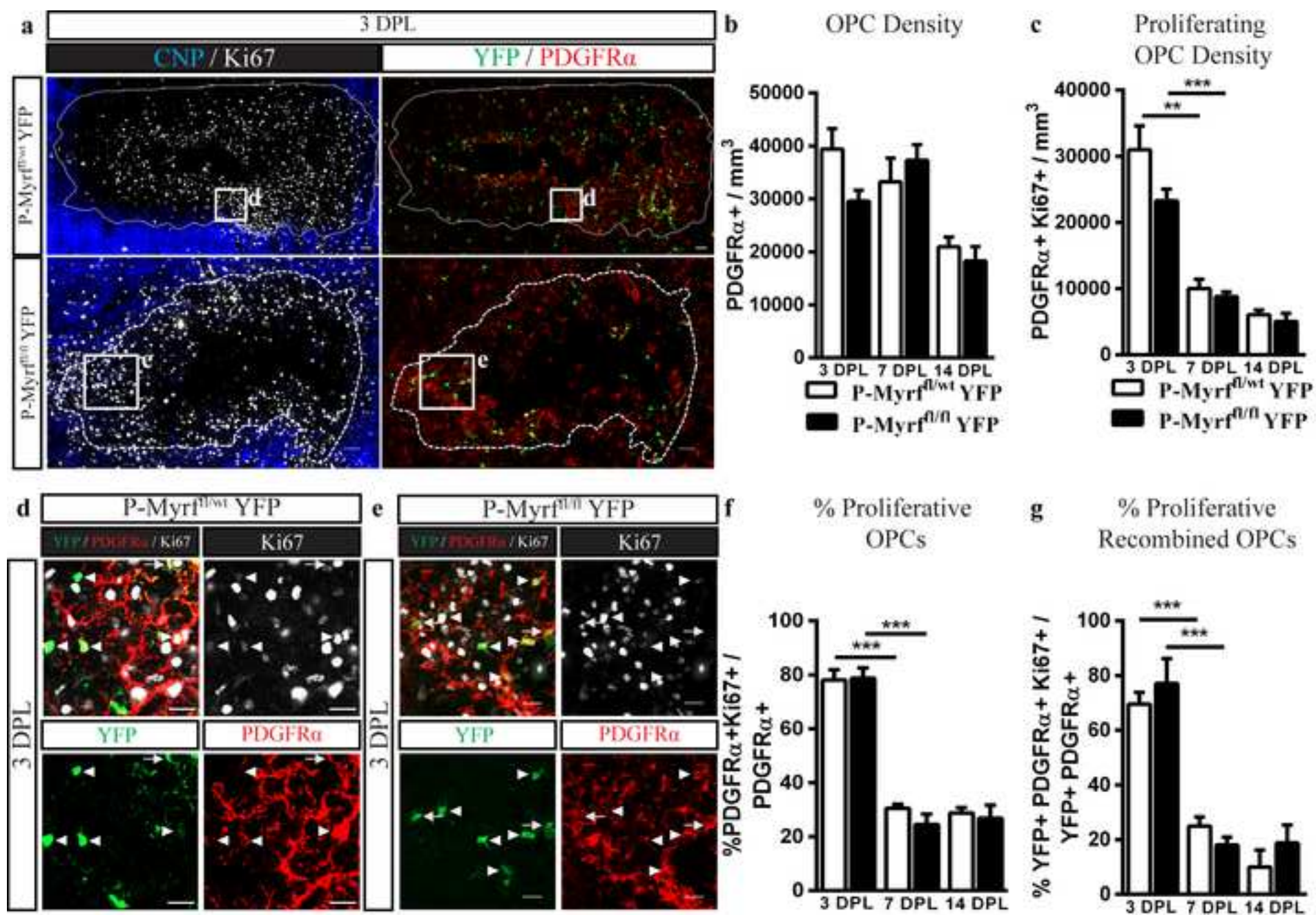843 sclerosis. Brain 123 (Pt 1): 105-115
844 63 Xiao L, Ohayon D, McKenzie IA, Sinclair-Wilson A, Wright JL, Fudge AD, et al. (2016) Rapid
845 production of new oligodendrocytes is required in the earliest stages of motor-skill learning. Nat
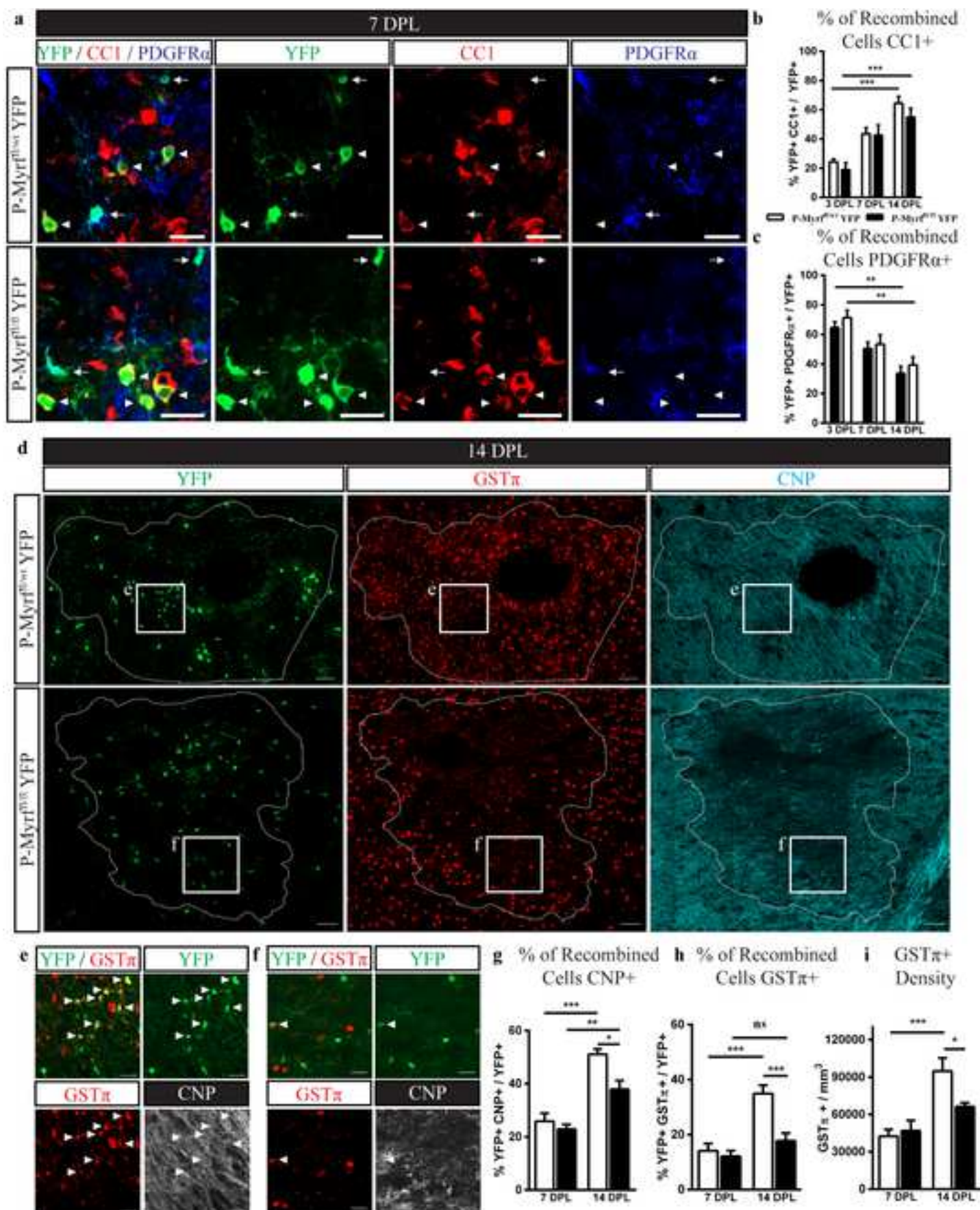846 Neurosci 19: 1210-1217 Doi 10.1038/nn.4351
847 64 Yeung MSY, Zdunek S, Bergmann O, Bernard S, Salehpour M, Alkass K, et al. (2014) Dynamics of
848 Oligodendrocyte Generation and Myelination in the Human Brain. Cell 159: 766-774 Doi
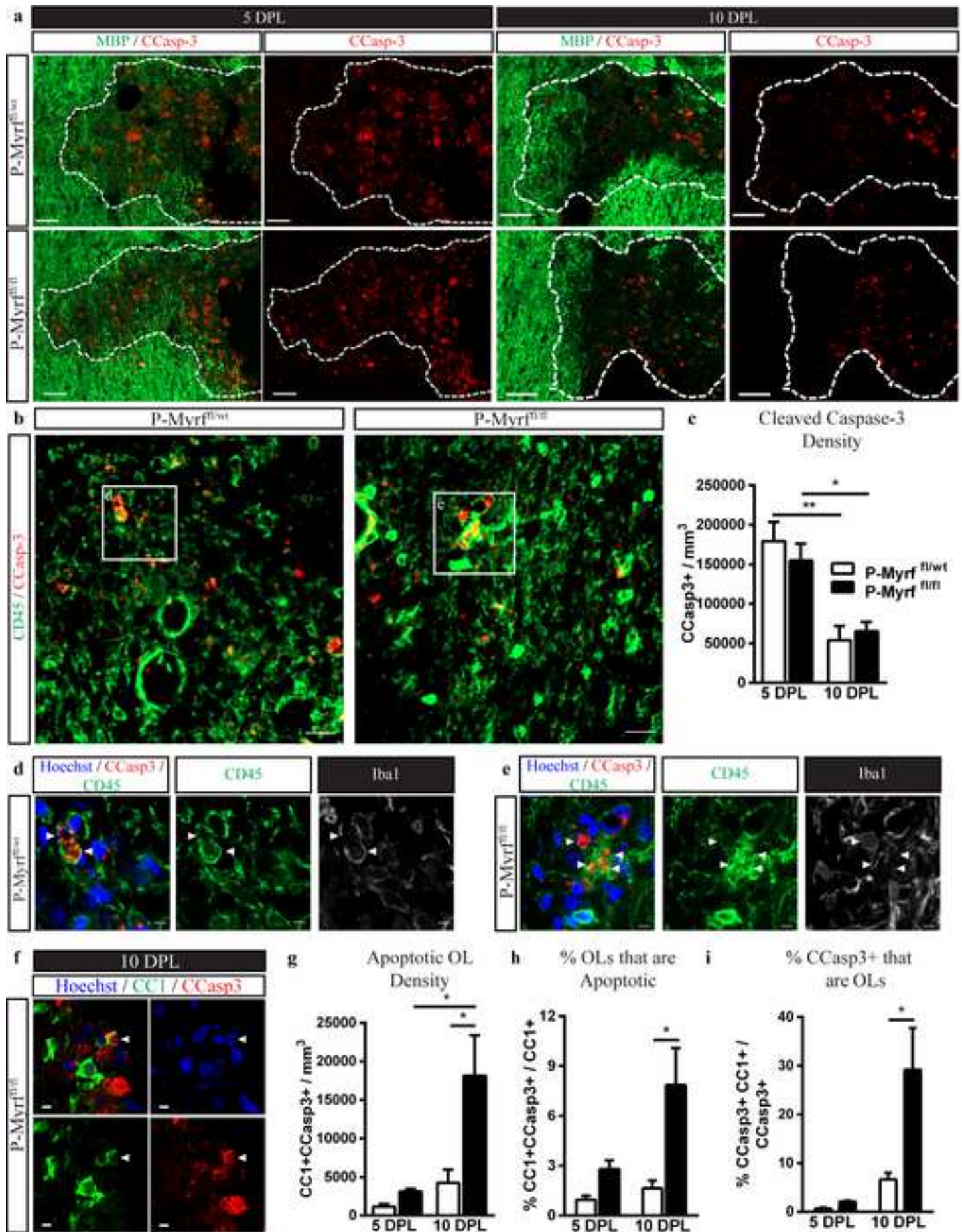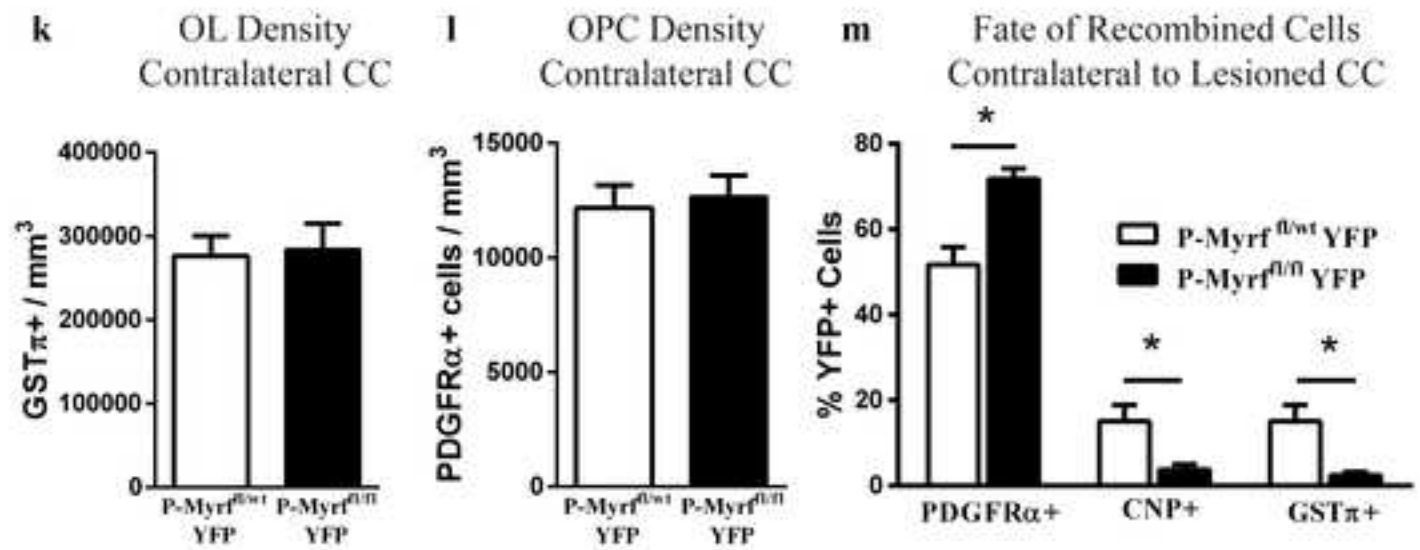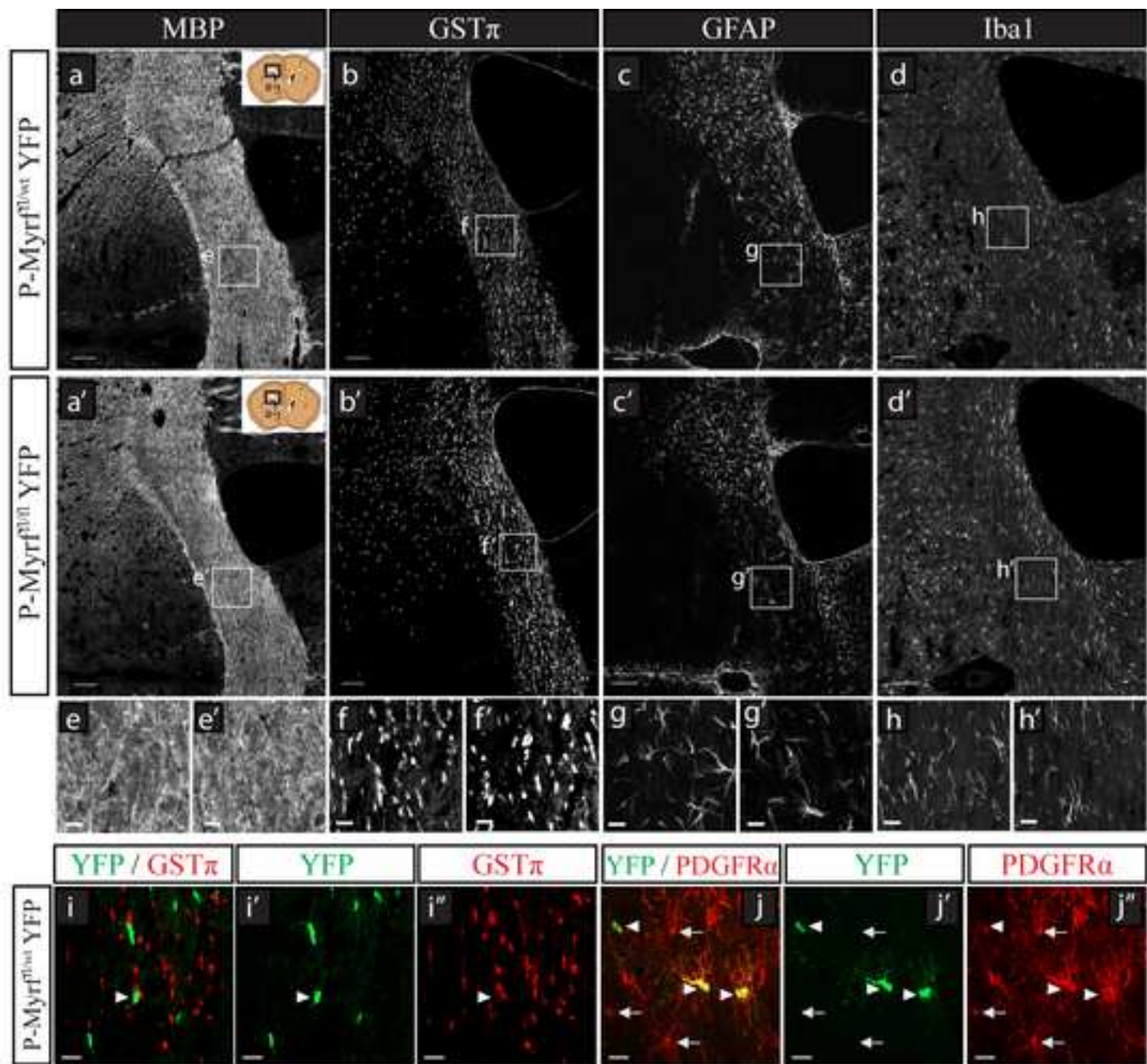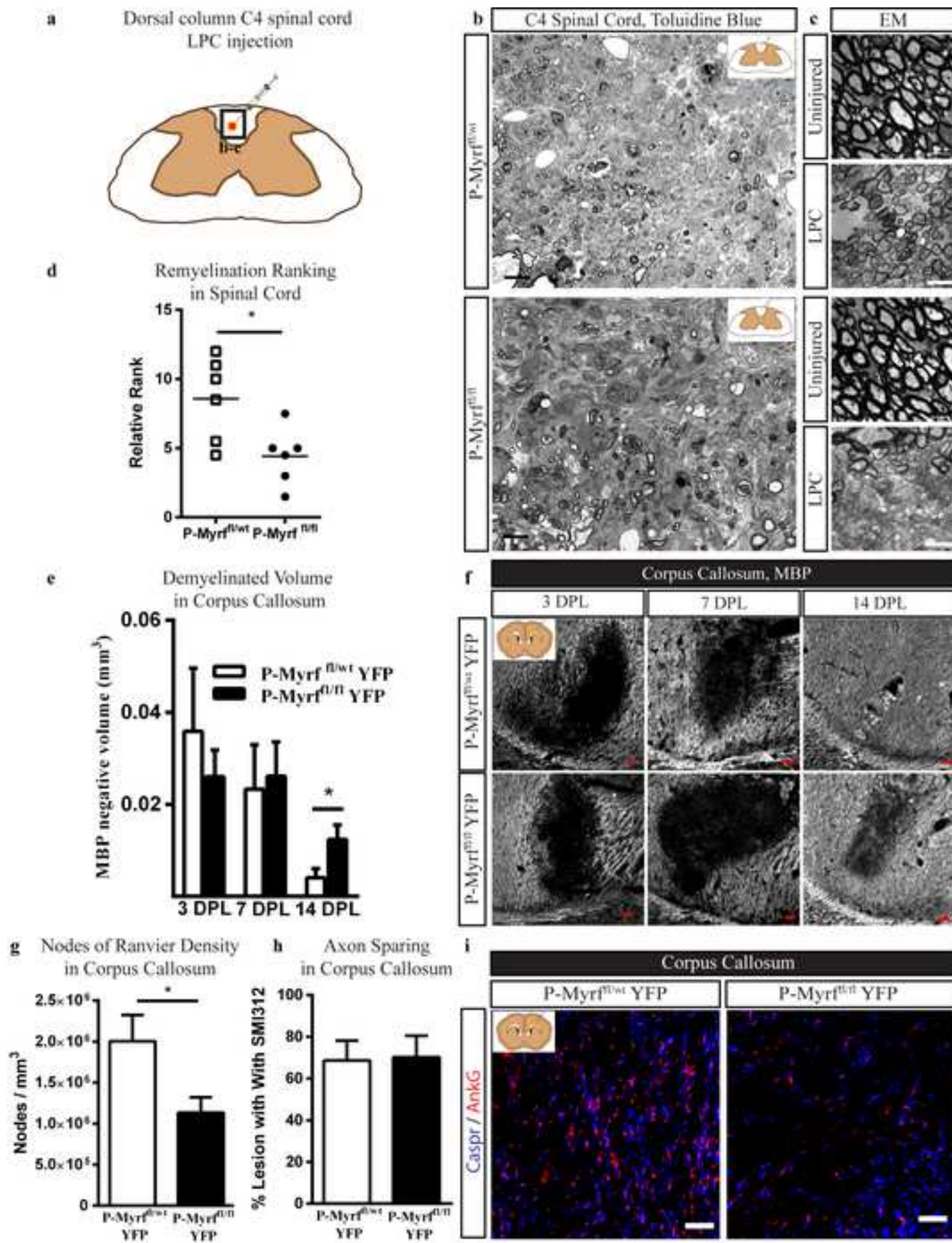849 10.1016/j.cell.2014.10.011

850

851

28

Fig1

Click here to download figure Fig1.tif ⬇

Fig1

Fig2

Click here to download figure Fig2.tif

Fig3

Fig4

Click here to download figure Fig4.tif ⬇

Fig5

Click here to download figure Fig5.tif

Fig5

Fig6

a Dorsal column C4 spinal cord LPC injection

b C4 Spinal Cord, Toluidine Blue

c EM

d Remyelination Ranking in Spinal Cord

e Demyelinated Volume in Corpus Callosum

f Corpus Callosum, MBP

g Nodes of Ranvier Density in Corpus Callosum

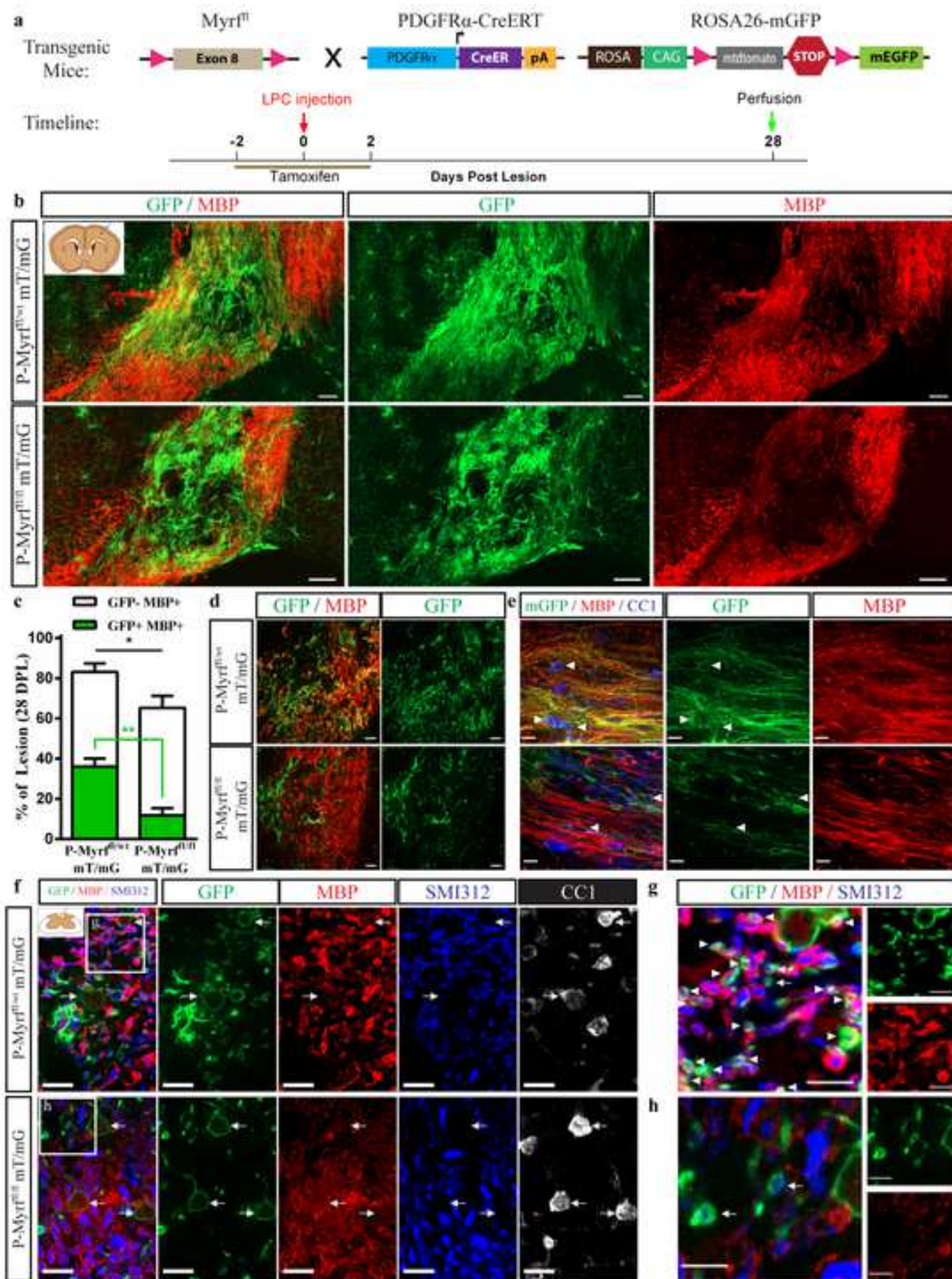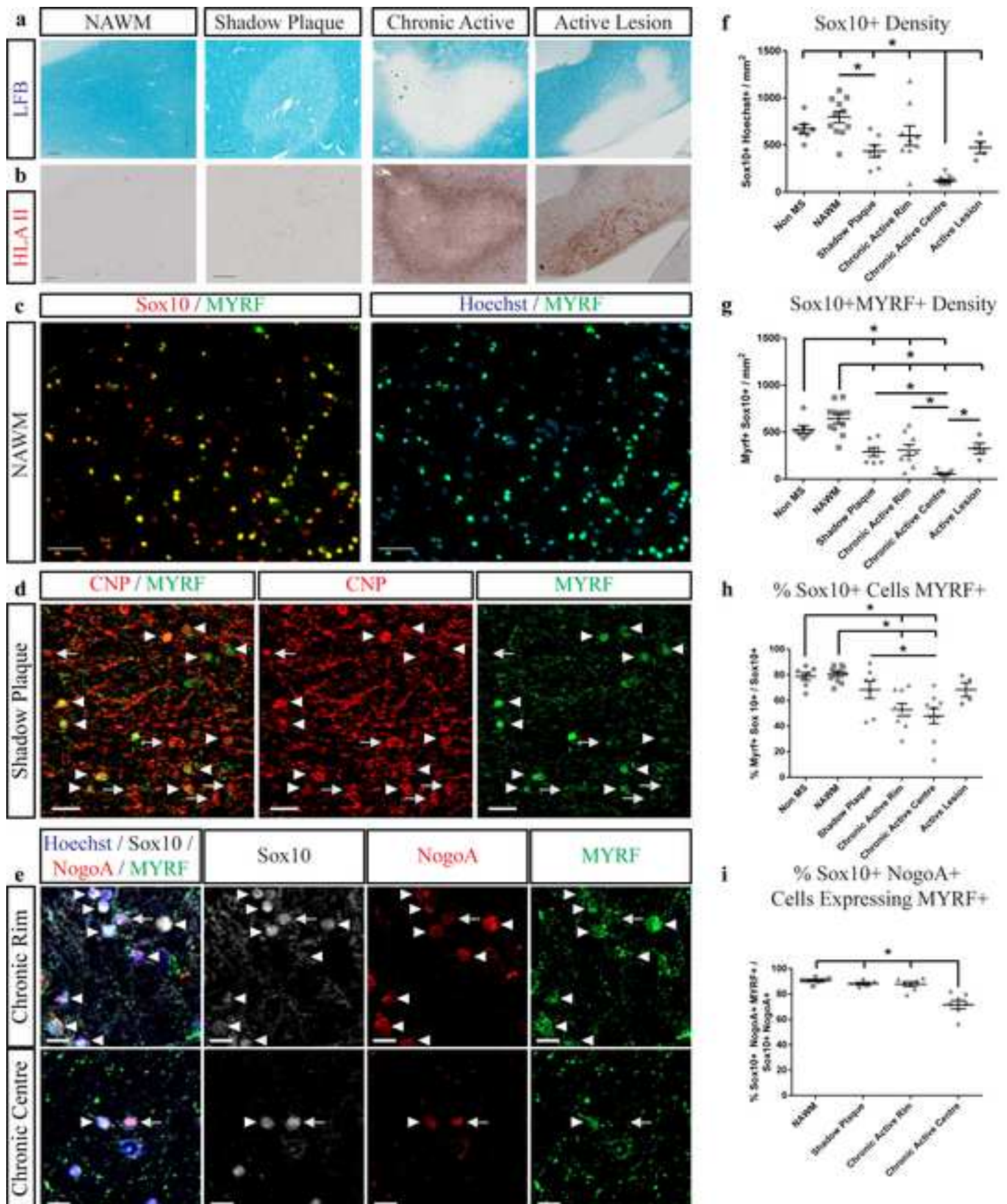**h** Axon Sparing in Corpus Callosum

i Corpus Callosum

Fig7

Fig8

Click here to access/download
electronic supplementary material
ESM.pdf